The Thesis Committee for Aleksandr Montelli
Certifies that this is the approved version of the following thesis:

Seismic stratigraphy and paleo-glaciology of Sabrina Coast, East Antarctica and Bering Trough, Gulf of Alaska

APPROVED BY
SUPERVISING COMMITTEE:

Supervisor: _____

Sean P.S. Gulick

_____

Donald Blankenship

_____

David Mohrig

Seismic stratigraphy and paleo-glaciology of Sabrina Coast, East Antarctica and Bering Trough, Gulf of Alaska

by

Aleksandr Montelli, B.S., M.S.

Thesis

Presented to the Faculty of the Graduate School of

The University of Texas at Austin

in Partial Fulfillment

of the Requirements

for the Degree of

Master of Science in Geological Sciences

The University of Texas at Austin

May 2015

Abstract

Seismic stratigraphy and paleo-glaciology of Sabrina Coast, East Antarctica and Bering Trough, Gulf of Alaska

Aleksandr Montelli, M.S. Geo. Sci.
The University of Texas at Austin, 2015

Supervisor: Sean P.S. Gulick

Examination of the sedimentary record in areas occupied by fast flowing outlet glaciers and ice streams is critical for understanding ice sheet dynamics on millennial timescales. We use high-resolution seismic data together with log data and foraminiferal-based radiocarbon and isotope data from Integrated Ocean Drilling Program (IODP) Expedition 341 cores to examine the evolution of the Cordilleran Ice Sheet (CIS) in southeast Alaska. Evidence for at least seven advances of the Bering Glacier to the shelf break since the end of Middle Pleistocene Transition (MPT) are interpreted from the seismic data. Seismic data demonstrate two distinctive patterns of slope sedimentation, which are: (1) dominated by sediments bypassing a steep paleo-slope or (2) dominated by glacigenic debris flows (GDFs) that form a trough mouth fan (TMF) on a lower slope. Integration of seismic, well, and age data suggests that the TMF was formed as a result of three advances to the shelf break since ca. 140 ka, implying extreme (average > 4m/ka) rates of sediment delivery. Extraordinarily high sediment flux played a key role in the development of the margin architecture resulting from a temperate, highly aggressive Bering Glacial System and abundant source of erodible bedrock onshore (St. Elias orogeny).

We use the first high-resolution seismic data acquired on the Sabrina Coast, East Antarctica, together with core data, to examine major transitions in glacial regime of East Antarctic Ice Sheet. Three large-scale megasequences represent changes in the dominant

pattern of sedimentation: Megasequence I shows signs of Eocene fluvial and possibly glacio-fluvial sedimentation; Megasequence II provides evidence of Oligocene-Miocene polythermal glacial sedimentation with significant amount of meltwater; Megasequence III overlies the regional erosional surface that marks major Miocene ice sheet expansion and transition into polar (cold- based) ice sheet glacial regime with no significant evidence of subglacial meltwater preserved. Megasequence II exhibits preserved record of EAIS evolution starting from its first expansion. Seismic stratigraphic analysis suggests a dynamic glacial late Paleogene-early Neogene evolution including expansions of the EAIS across the shelf at least eight times, which is marked by erosional surfaces and chaotic acoustic character of overlying strata. We report on finding the first conclusive seismic evidence of deep, extensive tunnel valley systems incised into sedimentary substrate from Antarctic continental margins. The Sabrina Coast tunnel valley system was presumably formed during Oligocene as a result of the second major EAIS shelf expansion. Shallower erosion events observed in the upper part of Megasequence II suggest more extensive glaciations in the Oligocene compared to the Miocene.

Table of Contents

Chapter 1: Introduction **1**
1.1. Paleo-glaciology: implications for understanding climate change **1**
1.2. Past ice sheets and glacial sedimentation: background **2**
1.3. Objectives **3**

Chapter 2: Late Quaternary glacial dynamics and sedimentation variability in Bering Trough, Gulf of Alaska **5**
2.1. Introduction **5**
2.2. Bering Temperate System, Gulf of Alaska **6**
2.3. Data and Methods **7**
2.4. Seismic Stratigraphy of Bering Trough **8**
2.5. Sedimentation and Glacial History of Bering Trough **9**
2.6. Discussion **11**
2.7. Conclusion **14**

Chapter 3: Seismic stratigraphy of the Sabrina Coast shelf, East Antarctica: history of early glaciation **15**
3.1. Introduction **15**
3.2. Data and Methods **16**
3.3. Background **17**
3.3.1 Geological background 17
3.3.2. Glaciological background 18
3.3.3 Sabrina Coast margin physiography and Cenozoic sedimentation 19
3.3.4 Antarctic Cenozoic glaciation 20
3.4. Bathymetry **21**
3.4.1. Observations 21
3.4.2. Interpretation 23
3.5. Seismic stratigraphy **26**
3.5.1 Seismic facies and morphological features 26
3.5.2 Large-scale shelf sequences composition: general overview 27
3.5.3 Units 1 and 2 30
3.5.4 Units 3-4-5 35
3.5.5 Units 6-7-8 36
3.6. Discussion **39**
3.6.1 Sabrina Coast tunnel valley system 39
3.6.2 Sabrina Coast shelf sedimentary architecture and Aurora Basin Complex paleodrainage 41
3.6.3 Early ice sheet dynamics in SC 42
3.6.4. Ice sheet dynamics in SC and linkages to global climate 43
3.7. Conclusions **45**
References **47**

Chapter 1: Introduction

1.1. Paleo-glaciology: implications for understanding climate change

Because many heavily populated areas are located along coastlines, future sea-level rise would have substantial societal and economic importance *(Alley et al., 2005)*. The largest recently observed contributions to the sea-level rise come from the ocean thermal expansion (0.8 mm/yr) and the melting of glaciers and ice caps (0.7 mm/yr) *(Church et al., 2011)*. While the actual sea-level rise observations are quite accurate, the projections for the next centuries show significant uncertainties, with potential contributions from land ice mass loss dominating these uncertainties *(IPCC, 2013)*. Therefore, while attempting to improve the accuracy of sea-level projections, it is essential to deepen our understanding of past climates and environments, particularly at high-latitude continental margins in both hemispheres *(Siegert et al., 1999; Zachos et al., 2001)*.

Paleoclimatological and paleoglaciological studies at polar margins have been largely using ice cores and sedimentary records. While ice cores can provide exceptionally well-preserved climate records in unparalleled temporal and spatial resolution *(e.g., Steffensen et al., 2004)*, they are not capable to give insights on paleoclimate older than 1 Myr. Unlike ice cores, sedimentary records at polar margins can help elucidate the dynamics of much more ancient paleoenvironments *(e.g., Naish et al., 2001),* providing the full context of Cenozoic climate change. Therefore, surficial processes at polar continental margins are critical to understanding the key linkages between glacial dynamics and climate change on millennial timescales *(Ottessen and Dowdeswell, 2006)*.

Despite recent advances in the understanding of glacial and sedimentary processes in polar regions, many margins, particularly those of Alaska, East Antarctica and northeastern Eurasia, are poorly constrained with relatively little being known about the sedimentary architecture and chronology of ice-sheet growth and decay *(Nielsen et al., 2005)*. Moreover, views on some important phenomena, e.g. formation of tunnel valleys, mechanisms of ice sheet collapse and impact of sedimentation on ice sheet stability, are matters of debate *(Alley et al., 2007; Lonergan et al., 2006)*.

1.2. Past ice sheets and glacial sedimentation: background

Ice sheets have repeatedly grown and decayed across continental shelves over Neogene in Greenland and Antarctica *(Elverhøi et al., 1998; Rebesco et al., 2006)* and Quaternary in the European and North American Arctic *(Butt et al., 2001; Batchelor et al., 2012)*. Most ice sheet drainage and mass loss is released through outlet glaciers *(Dowdeswell, 2006)* and fast flowing ice streams *(Shepherd and Wingham, 2007)*, which exert a significant impact on ice sheet stability and have the potential to trigger hemispheric climate change through catastrophic discharge of fresh meltwater *(Clark et al., 2003; Tarasov et al., 2005)*. Ice streams represent narrow (tens of kilometers wide) areas of rapid ice flow confined within slower inter-ice stream regions. Recurrent expansions of ice streams have resulted in development of deep (hundreds of meters) and wide (up to few tens of kilometers) cross-shelf troughs, which in most cases terminate at the shelf break *(Dowdesell and O'Cofaigh, 2002)*. Advancing to the shelf break, ice streams provide a focused delivery of sediments to the continental slope during full-glacial periods *(Batchelor and Dowdeswell, 2014)*.

Various factors control the rates of glacial sediment delivery, most importantly timespan of the ice age resulting from orbital forcing, rates of ice flux and subglacial conditions, including erodibility of the source, as well as tectonics and isostasy *(e.g., Blankenship et al., 1986; O'Cofaigh et al., 2003; Berger et al., 2008; Jamieson et al., 2010; O'Cofaigh et al., 2013; Swartz et al., 2015)*. Although sedimentation rates vary across different glaciated margins, they are generally an order of magnitude higher than those exhibited by the largest fluvial basins, such as the Mississippi or Amazon rivers *(Elverhoi et al., 1998; Dowdeswell et al., 2010)*. In cases when continental-slope gradients are low (generally accepted to be less than 4°) high rates of sediment delivery favor the development of vast fans located on the slope *(O'Cofaigh et al., 2003)*. These thick piles of sediments (1 km or more), composed mainly of reworked tills deposited in the form of glacigenic debris flows, are called trough-mouth fans (TMFs) *(Vorren et al., 1997)* and are of particular importance for paleo-glaciological reconstructions, providing a record of glacial dynamics and sedimentation over the past few million years.

Periods of ice sheet advance and retreat affect the sedimentary architecture of adjacent shelf/slope systems, leaving a number of morphological features diagnostic of

past glacial processes in the sedimentary record of the margin. These landforms, such as grounding-zone wedges, till sheets, subglacial meltwater tunnel valleys, drumlins, gullies, mega-scale glacial lineations, provide important indicators of past glacial dynamics, including the extent of glacial advances, the style and rate of glacial retreat, subglacial conditions (e.g., polythermal versus cold-based regimes) and changes in paleo-ice stream flow directions *(e.g., Dowdeswell et al., 2007; Laberg et al., 2010; Batchelor et al., 2013)*.

Thus, reconstructions of past ice sheets are generally studied using geophysical and sedimentological data. Seismic data in particular represent a powerful tool for morphologic and stratigraphic interpretations and can help to delineate a range of erosional and depositional processes that occur beneath and proximal to ice sheets. Swath-bathymetric data facilitates the understanding of processes related to the most recent glacial retreat and constrains the Last Glacial Maximum (LGM) extent of ice sheets, whereas drilling and core data are necessary to put the history of glacial dynamics in the global chronological context as well as reliably determine past depositional environments.

1.3. Objectives

Since this study uses data from two completely different areas, this study can be split into two subprojects. Major objective of the first is to improve our understanding of previously studied Bering Trough, Gulf of Alaska continental margin and reconstruct the configuration, extent and dynamics of the marine part of Cordilleran Ice Sheet in Late Quaternary. The second part aims at examining the sedimentary record and glacial history of previously unstudied Sabrina Coast shelf, East Antarctica. These objectives are accomplished using integration of high-resolution marine geophysical and sedimentological data acquired in both regions.

In general, research questions that drive this project are:

a) What is the extent and number of ice advances across the shelf that occurred on each margin and what correlation exists with the global and regional climate oscillations?

b) Were the overall dynamics of the ice stream/ice sheet in phase with global ice sheets fluctuations?

c) How did the glacial system impact the sedimentary architecture of the margin?

d) How did the glacial regime evolve through time (e.g., polythermal-polar transitions)?

e) What are the implications for constraining ice sheet numerical modelling and global climate change projections?

Chapter 2: Late Quaternary glacial dynamics and sedimentation variability in Bering Trough, Gulf of Alaska

2.1. Introduction

Marine terminating outlet glaciers and ice streams dominate mass transfer and discharge from ice sheets and are critical components of associated sea level rise *(Stokes et al., 2014)*. Understanding the past chronology and configuration of such glaciers is essential to constrain numerical models and predict future feedbacks between the behavior of contemporary ice sheets and climate change *(Siegert et al., 1999)*. Direct observations of ice sheets and their drainage systems are limited to the past few decades, so studying the geologic record is necessary to understand the dynamics and behavior of past ice sheets on centennial to millennial timescales *(Briner et al., 2009)*.

Recurrent expansions of ice streams during periods of ice sheet growth and decay have resulted in the development of deep (hundreds of meters) and wide (up to few tens of kilometers) cross-shelf troughs on glaciated continental margins, which in most cases terminate at the shelf break *(Carlson, 1989; Batchelor et al., 2013)*. Advancing to the shelf break, ice streams deliver large volumes of sediment to the continental slope, commonly forming diamict-dominated trough mouth fans (TMFs) that are useful indicators of paleo-ice streams *(O' Cofaigh et al., 2003)*.

Seismic stratigraphy of marine glaciated margins has been widely used to evaluate architecture of high-latitude margins as well as the extent and dynamics of glaciers and ice sheets in the past *(e.g., Powell and Cooper, 2002; Elmore et al., 2013; Batchelor et al., 2013)*. Although numerous geophysical investigations have been performed on high latitude margins in both hemispheres, studies that have examined glacial history by integrating chronostratigraphy from deep drilling cores with high-resolution seismic data are rare *(e.g., Laberg et al., 2010)*. In this paper we use high-resolution seismic and IODP Expedition 341 drilling data from a tectonically active margin in the Gulf of Alaska to examine paleo-glaciology of the northwest CIS and the sedimentary architecture of the adjacent margin.

2.2. Bering Temperate System, Gulf of Alaska

In Southern Alaska, the St. Elias orogen was formed as a result of ongoing oblique collision of the Yakutat oceanic plateau and North American plate initiated in middle Miocene *(Plafker et al., 1994; Christeson et al., 2010).* By Late Miocene - Early Pliocene, the convergence built topography high enough to trap heavy orographic precipitation and trigger one of the most extensive tidewater glaciations in the world *(Lagoe et al., 1993).* Previous studies have divided the history of glaciation into three distinct phases *(Lagoe et al., 1993)*. The latest of which, glacial interval C started ~1 Myr ago possibly as a result of the mid-Pleistocene transition (MPT) from 41 kyr to 100 kyr dominated glacial cycles (e.g., *McClymont et al., 2013*) and associated intensification of Northern Hemisphere glaciation *(e.g., Berger et al., 2008; Jaeger et al., 2014)*.

Northern Gulf of Alaska shelf bathymetry exhibits several cross-shelf troughs developed during periods of glacial advance as a result of erosion associated with focused ice flow. One of these troughs, the 25 km wide and 55 km long Bering Trough (Fig. 2.1) was formed as a result of Late Pleistocene erosional activity of Bering Glacier *(Carlson, 1989).* With a modern drainage area of 5175 km^2, Bering Glacier accounts for about 15% of glacier ice in Alaska and is the largest existing temperate glacier *(Molnia, 2010).* During periods of glaciation, it coalesced with adjoining glaciers and ice fields, draining the northern part of CIS *(Briner and Kaufman, 2008).* The tectonic and structural evolution of the Bering Trough region have been previously investigated *(e.g., Plafker et al. 1994; Berger et al., 2008; Worthington et al., 2010)*. However, little is known about the timing of glaciations throughout the middle to Late Pleistocene on millennial timescales because of the lack of timing constraints prior to Expedition 341 drilling. Here we examine the sedimentary record of the Bering Glacier, constrain number, timing and extent of glacial advances across the Bering Trough in the Late Quaternary, and discuss impact of the Bering Glacier's activity on the architecture of adjacent shelf and slope.

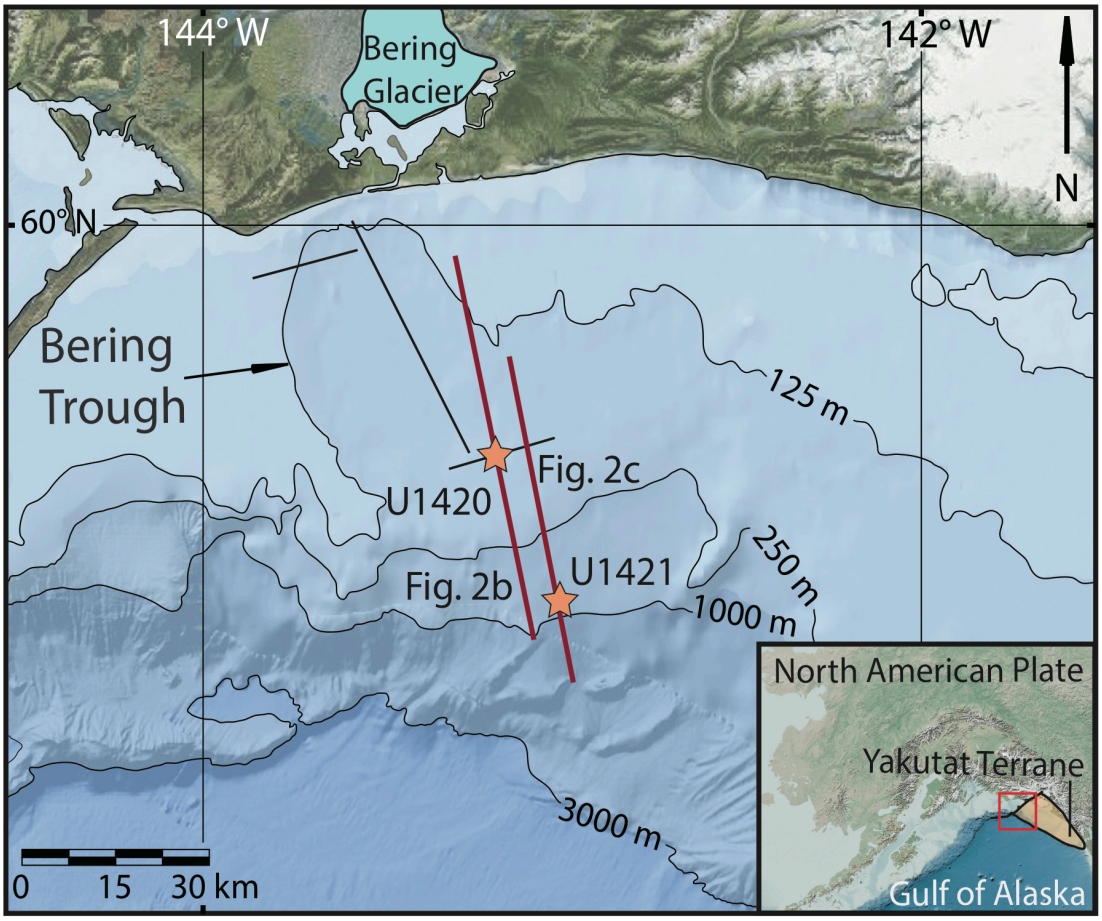

Figure 2.1. Shaded relief map of northeast Gulf of Alaska showing Bering Trough. Lines indicate seismic profiles. Orange stars show locations of IODP 341 drilling sites.

2.3. Data and Methods

Approximately 1800 km of high vertical resolution (3-5 meters) multichannel seismic data shot with dual 45/45 in^3 GI airguns were acquired in 2004 *(Gulick et al., 2007).* Two-way travel time seismic profiles were used for the seismic stratigraphic interpretation of the region. Processing included trace regularization, normal moveout correction, bandpass filtering, muting, f-k (frequency-wave number) filtering, stacking, water-bottom muting, and finite-difference time domain migration *(Gulick et al., 2007).*

This study uses cores and logs acquired by IODP Expedition 341 from drill sites U1420 and U1421 located on the shelf and slope of Bering Trough, respectively (Fig. 2.1). Radiocarbon and oxygen isotope analyses of planktic and benthic foraminifera provide chronostratigraphic control for ages of the strata at site U1421. A vertical seismic

profile log from site U1421 was used to calibrate borehole depth to the two-way travel time of the seismic data and correlate ages with interpreted horizons. Shipboard biostratigraphic analysis, paleomagnetic data, and seismic correlation provide a preliminary chronology for site U1420.

2.4. Seismic Stratigraphy of Bering Trough

Powell and Cooper *(2002)* previously examined seismic architecture and lithofacies of the upper 500 meters of the Bering Trough, interpreting three erosional surfaces including the regional unconformity (hB1 in this study, Fig. 2.2). Based on correlation with biostratigraphic data Berger et al. *(2008)* suggested that this unconformity was formed as a consequence of the MPT. Worthington et al. *(2010*) analyzed the complete section and suggested that the regional unconformity (hB1) divides the sedimentary succession of the Bering Trough into two distinctive packages that reflect waning deformation prior to and cessation of deformation after the event associated with regional erosion.

This study refines previous interpretations with updated chronology from IODP Expedition 341 and detailed seismic facies descriptions within the Bering Trough. We distinguish five main seismic facies based on previous seismic and lithostratigraphic studies of glaciated margins globally (Fig. 2.2A) (*e.g., Carlson, 1989; Cai et al., 1997; Batchelor et al., 2013).* These facies characterize ten separate units within the upper 2000 meters, which, in turn, comprise two larger sequences, A and B, differentiated by an architectural shift in margin structure (Fig. 2.2).

We suggest that chaotic, transparent facies, *C,* all located above erosional unconformities represents layers of subglacial till *(e.g., Dowdeswell et al., 2004; Batchelor et al., 2013)*. Irregularly channelized, mounded, internally chaotic facies *M* represents recessional morainal banks formed during periods of short stillstands of glacier retreat and are analogous to those formed in other areas dominated by tidewater glaciers *(e.g., Powell and Cooper, 2002; Ottessen and Dowdeswell, 2006).* Well-stratified, continuous, high-amplitude facies *S* is interpreted as ice distal sediments deposited in open marine conditions during interglacial stages. Facies *O* reflects sediments that onlap the slope, with semi-continuous stratification and gently mounded configuration. We suggest that Facies O sediments bypass the slope in the form of turbidity currents, ice-

rafted debris, and settling from meltwater plumes *(O' Cofaigh et al., 2003)*. Stacked transparent lenses bounded by stratified laminated reflectors on the slope define facies *L* interpreted as reworked glacigenic sediments that were deposited on the slope forming TMF. Discontinuities in facies *L* are interpreted as slide scars, providing evidence for multiple events, potential hiatuses, and associated submarine sliding and slope failures. Thin, acoustically stratified reflectors bounding subunits within the TMF represent ice distal sediments deposited during periods of glacial retreat associated with Facies S *(e.g., Laberg et al., 2010)*.

Sequence A is composed of six units (A.1-A.6), each up to 250 m thick, bounded by truncating reflectors interpreted as erosional surfaces that mark advance of the glacier to the shelf break. Units A.1-A.6 demonstrate a systematically similar pattern of sedimentary deposits, in terms of both geometry and seismic facies. These units are composed of facies *M,* in places underlain by facies *C* on the shelf and are dominated by facies *O* on the steep (~10°) paleo-slope (Fig. 2.2B). Unit A.7 is dominated by facies similar in reflection character to facies *O*. However, unit A.7 is truncated by the surface hB1, which doesn't allow us to examine its origin and is, therefore, interpreted to represent a transition from bypass dominated sedimentation to slope sedimentation and formation of a TMF. Units B.3-B.1 are bounded on the shelf by erosional surfaces and consist of three major seismic facies *S, C* and *L*. Shelf sediments of sequence B are mainly composed of facies *S* and thick successions of facies *C*. Slope sediments are composed entirely of facies L suggesting the development of TMF (Fig. 2.2C).

2.5. Sedimentation and Glacial History of Bering Trough

Cores recovered from Site U1421 are dominated by grey to very dark grey clast-rich and clast-poor diamict with intervals of dark grey to dark greenish grey mud with occasional presence of lonestones *(Jaeger et al., 2014)*. Correlation of major reflectors on the slope with ages inferred from Site U1421 allows estimation of the timing of TMF formation as well as millennial-scale advance-retreat cycles of Bering Glacier through at least last 5 Marine Isotopes Stages (MISs). Radiocarbon data from the upper 220 m of site 1421 imply average slope sedimentation rates of 5.9 m/ka starting from ca. 39 ka and show two age reversals that likely result from abundant slope slumping and sliding observed in the seismic data (Figs. 2.2D and 2.3C). The highest sediment flux of 10.7

m/ka was sustained between ca. 38 and 28 ka (Fig. 2.3C). Oxygen isotope data suggest that the horizon representing the base of the TMF matches the low in $\delta^{18}O$ values that could represent either MIS 5e or MIS 7. However, the latter case would imply at least one additional significant erosional event associated with MIS 6, for which there is no seismic evidence. We therefore suggest that the TMF was formed during three phases of erosion starting ~130 ka. Assuming that this scenario is correct, the average sedimentation rate at U1421 for sequences B.1-B.3 is > 4 m/ka.

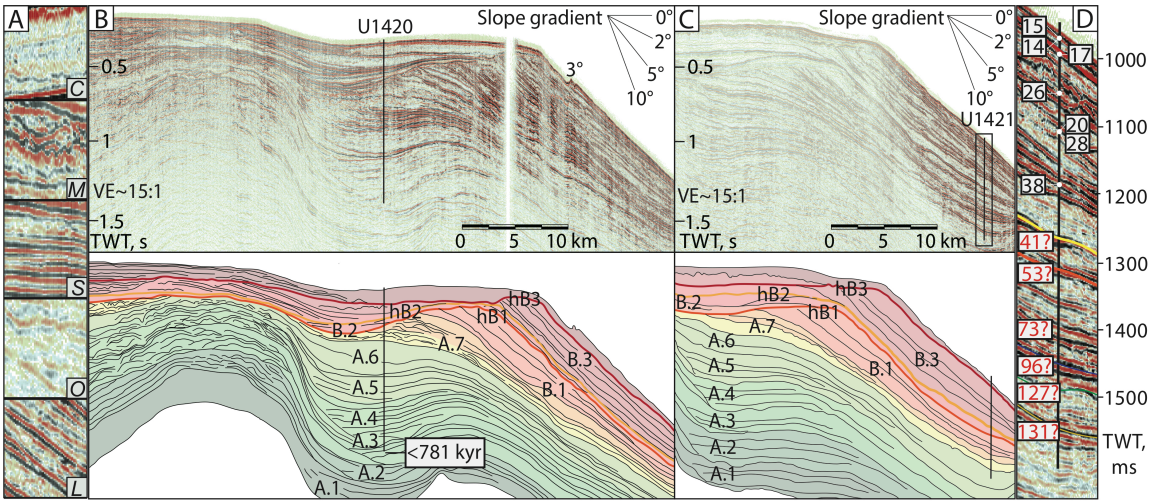

Figure 2.2 A: Five seismic facies identified from the seismic data in the Bering Trough: C-chaotic, internally transparent; M-mounded, hummocky; S-stratified, laminated; O-onlapping, semi-continuous; L-lobate, oblique, internally transparent. B: Seismic dip profile goa2505 showing shelf and slope architecture of Bering Trough and sequence interpretation. C: Seismic dip profile goa2503 showing sequence interpretation. D: Correlation of well U1421 with seismic line goa2503. Radiocarbon ages (in black font) and oxygen isotope ages assuming low $\delta^{18}O$ correspond to MIS 5e (in red font).

Low core recovery from Site U1420 does not make it possible to establish the detailed history of evolution of units comprising sequence A. However, the deepest core, recovered from depth of 1020 m is still normal magnetic polarity and thus is younger than the Bruhnes-Matayama paleomagnetic boundary (~0.781 Ma). This core is also older than ~0.3 Ma based on preliminary biostratigraphy *(Jaeger et al., 2014)*. These age data suggest that advances related to units A.4 and younger occurred after the Bruhnes-Matayama reversal (Fig. 2.2C). Thus, all recovered sediments in U1420 and U1421 are

younger than the end of the MPT and were deposited in a 100 kyr glacial cycle dominated world (*McClymont et al., 2013*).

2.6. Discussion

Analysis of Bering Trough architecture shows a distinctive evolution from tectonically to depositionally controlled continental margin strata formation. Tectonic controls include the subduction of the Yakutat terrane beneath North American Plate, which creates significant offshore accommodation space adjacent to the Bering Glacier, and active deformation from a fold-and-thrust belt creating topography that influences tidewater glacial sedimentation. We suggest that this excess of accommodation space created sufficient water depth to prevent grounded ice from advancing into deeper water due to iceberg calving. Similarly, steep slope gradients (about 10°) limited slope sedimentation and facilitated sediment bypass to deeper waters *(e.g., O' Cofaigh et al., 2003).* The dominant facies onlapping the slope during this period is interpreted as sediments bypassing in the form of turbidity currents with a significant component of vertically deposited ice rafted debris (IRD) (Fig. 2.3A). During the development of sequence A, glacimarine and gravity sedimentation seaward of the anticline-caused upper slope proved rapid enough to fill the accommodation space between an inner and outer anticline (Fig. 2.2B). The accommodation space was filled by ca. 130 ka, significantly decreasing the slope gradient to <3° and effectively widening the continental shelf (Fig. 2.3). This transition was a fundamental autogenic shift in margin strata formation that allowed the grounded tidewater glacier terminus to subsequently advance farther seaward, eroding and reworking existing Sequence A glacimarine strata, and depositing stacked glacigenic debris flows (GDF) on the newly developing continental slope (Fig. 2.3B). This infilling also provided the change in normal stress to retard additional deformation within this portion of the fold-and-thrust belt, as noted previously by Worthington et al. (2010) although over significantly shorter timescales.

Sequence B was formed under these different conditions (Fig. 2.3B). Deposition of GDF during stages B.1-B.3 allowed the shelf break to prograde ~20 km farther offshore then its previous position. This advance resulted in the mature modern TMF similar in configuration to that observed at classical high-latitude passive margins *(e.g., Vorren and Laberg, 1997; O'Cofaigh et al 2003; Batchelor et al., 2014).* Thus, sequence

B was dominated by sedimentation and TMF build up on the new slope during glacial advance and subglacial till and morainal bank formation on the shelf during retreat or stillstand.

Margin tectonics and sediment supply to high-latitude continental slopes have been recognized as a key parameter controlling the architecture of glaciated margins *(O' Cofaigh et al., 2003).* Tectonically active margins with steep slopes tend to favor frequent gravity flows and development of a gulley, apron morphology. From a sediment supply perspective, the following factors favor high rates of sediment delivery that lead to the development of TMFs *(O' Cofaigh et al., (2003), Dowdeswell et al., (2010) and Batchelor et al., (2014))*: (1) long history of glaciations, (2) thicker and faster flowing ice, (3) low slope gradients (<4°) and passive tectonic setting, (4) wide, erodible continental shelf, (5) large drainage basin area, and (6) non-significant slope mass-wasting. The Bering Trough region is a tectonically active margin with initially steep slopes, a narrow continental shelf (~50 km) and a small drainage area, but the rapid infilling of tectonic accommodation and formation of a prominent, 600-meter thick Bering TMF deposited in <130 ka emphasizes the overriding importance of sediment flux in the evolution of the Bering Trough margin and we suggest glaciated tectonically active margins generally.

Our results confirm that extreme sedimentation rates observed in the Bering Trough are likely to represent a consequence of the proximal, active St. Elias orogen being successively eroded by highly aggressive temperate Bering Glacier System (*Sheaf et al., 2003; Swartz et al., 2015*). We suggest that glacial regime and a voluminous onshore sediment source must be considered among the factors that can significantly impact sediment flux to the continental margin producing the distinctive and common glacial slope deposits (TMFs) found in the geologic record.

Refined chronologies from Site U1421 suggest that the glacial advance associated with hB1 ceased by ca. 50 ka. This result contrasts with previous hypothesis of hB1 having been formed as a result of glacial intensification associated with the MPT and the inception of a large, long-lived ice stream *(Berger et al., 2008).* Our analyses show that the prominent character of erosional surface hB1 represents a fundamental shift in margin sedimentation that resulted from autogenic filling of accommodation space and lowered slope gradients rather than an allogenic change in climate regime and/or eustacy.

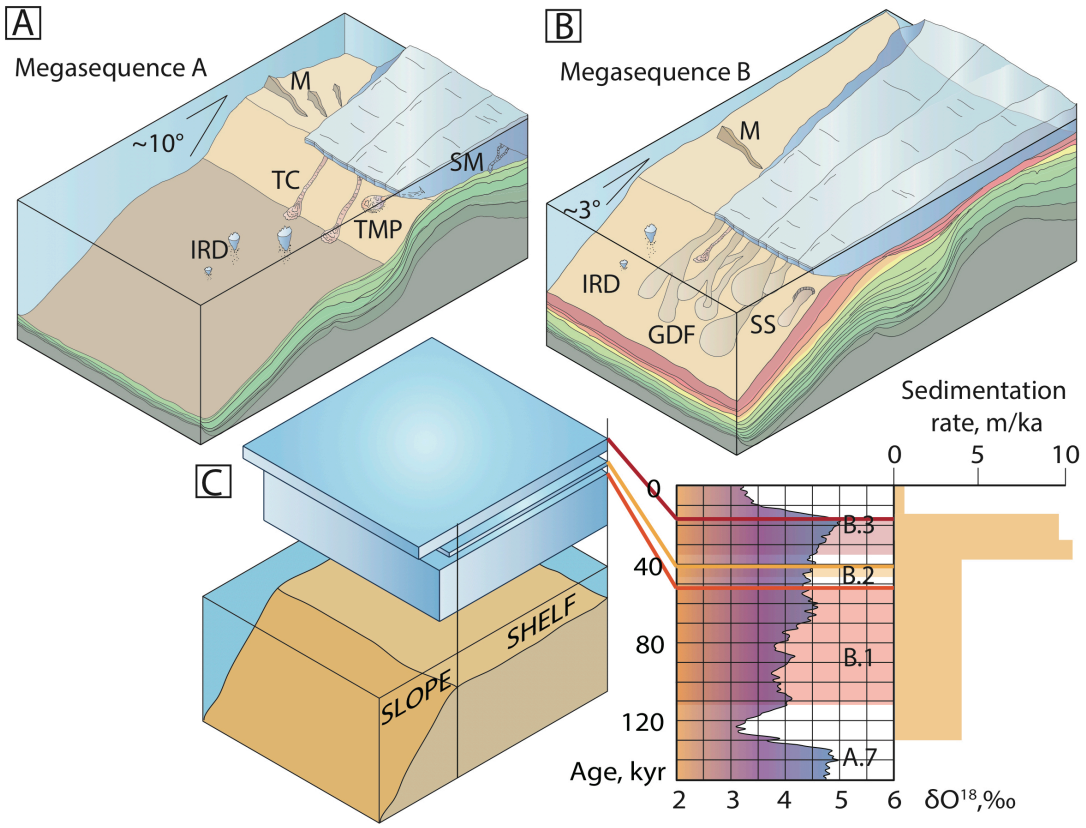

Figure 2.3. Conceptual model of Bering Trough slope sedimentation based on seismic data interpretation and the model by O'Cofaigh et al., (2003). A: Sedimentation processes dominated formation of megasequence A (pictured at the formation of A.5): steep slope (~10°) facilitates sediment bypass in form of: TC – turbidity currents; TMP – settling from meltwater plumes; IRD – ice rafted debris. Formation of moraines (M) and subglacial meltwater (SM) channels are shown to illustrate shelf processes during the retreat phase. B: Sedimentation processes dominated formation of megasequence B (pictured at formation of B.3): lowered slope (~3°) allows for slope deposition and formation of TMF. SS – slumps and slides, GDF – glacigenic debris flows on the slope. C: History of glacial advances and sedimentation rates versus global oxygen curve (modified from Lisiecki and Raymo, 2005) through last 5 MISs.

Comparison of sedimentation rates at the site with global ice volume *(Lisiecki and Raymo, 2005)* as a proxy suggests higher slope sediment flux during major glacial periods and lower rates during interglacials since MIS 6, which is likely the result of glacial growth and associated increase in ice flux to the continental slope. For example

the radiocarbon constrained 10.7 m/kyr interval from 38-28 ka amply emphasizes this point of maximum slope accumulation rates in a TMF during glacial maxima.

2.7. Conclusion

Since the MPT, the Bering Glacier has advanced to a temporally evolving shelf break at least seven times. Extreme rates of sediment flux played a key role in shaping the variable architecture of the margin. By ca. 130 ka, the Bering Glacier sediment delivery filled the tectonically created accommodation space, lowering slope gradients, and allowing for rapid tidewater glacier terminus advance and corresponding shelf progradation. Since 130 ka, the Bering Glacier has advanced to the prograding shelf break three times, delivering reworked glacigenic sediments at average rates of 4 m/ka to the continental slope. The presence of a prominent TMF on a narrow shelf on a tectonically active margin suggests that consideration of glacial regime and source volumes onshore are among the key factors controlling sedimentary architecture of glaciated margins.

Chapter 3: Seismic stratigraphy of the Sabrina Coast shelf, East Antarctica: history of early glaciation

3.1. Introduction

Antarctic Ice Sheets (AISs) have been a key element of the Cenozoic global climate system, exerting a strong influence on sea-level change and patterns of oceanic and atmospheric circulation *[Flower and Kennett, 1994; Close et al., 2007]*. Deciphering long-term record of Antarctic glaciations is thus essential to understand the fundamental changes in global climate on different scales, such as long-term greenhouse-icehouse transition and shorter-scale aberrations, and to help better project future changes in climate *[Zachos et al., 2001; Rebesco et al., 2006; Francis et al., 2008]*.

In the last two decades, major efforts have been made to scrutinize the glacial history of potentially unstable and largely marine-based West Antarctic Ice Sheet (WAIS) on different timescales *[e. g., Rignot et al., 1998; Shipp et al., 1999; Conway et al., 1999; De Angelis and Skvarca, 2003; Larter et al., 2014]*. Fluctuations of the larger, mostly land-based East Antarctic Ice Sheet (EAIS) have received less attention *[Bart et al., 2000]*. However, both numerical modeling and geophysical studies indicate that some parts of EAIS that are located below sea-level have played a significant role in the dynamics of the ice sheet and its impact on sea-level *[Siegert et al., 2005; Rignot et al., 2008; Pritchard et al., 2009; Young et al., 2011]*.

One such area within the EAIS, is the vast, deep Aurora Basin Complex (ABC), which is drained by mainly Totten Glacier (TG) and Moscow University Ice Shelf (MUIS) (Fig. 3.1), and currently shows negative mass balance *[Zwally et al., 2005; Pritchard et al., 2009; Rignot et al., 2011]*. Results of recent onshore geophysical surveys have suggested that ABC has experienced multiple glacial advances and recessions throughout Late Eocene to Middle Miocene, largely as a response to the orbital oscillations *[Young et al., 2011]*. Despite the existence of studies onshore and on the slope, the entire shelf context for the dynamics of ASB was absent until recently, when marine geophysical and geological data from the Sabrina Coast were acquired.

High-resolution seismic and bathymetry data collected on the shelf adjacent to MUIS provide a unique opportunity, for the first time, to elucidate late Paleocene-early

Neogene glacial history of one of the major drainage outlets of the deepest ice basin in Antarctica and to examine the sedimentary architecture of the adjacent continental shelf. The objectives of this study were to: (a) constrain the number of major glaciation events that have occurred since the onset of East Antarctic Ice Sheet (EAIS) expansion, (b) examine the impact of the glaciations on the continental shelf, and (c) resolve late Paleogene - early Neogene trends of EAIS dynamics and their relation to global climate patterns.

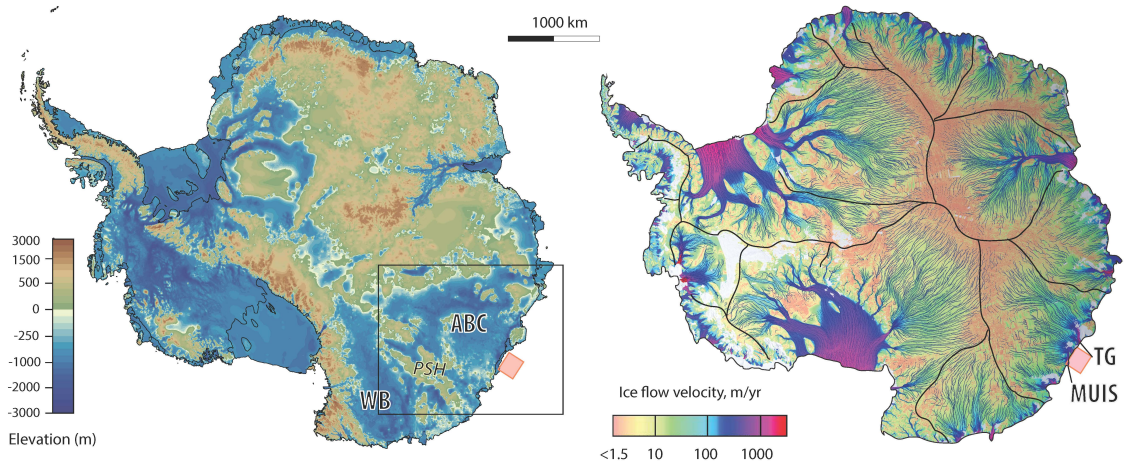

Fig. 3.1. To the left: bed topography of Antarctica (modified from BEDMAP2 data from Fretwell et al., 2013). Major elements of Wilkes Land are shown: ABC-Aurora Basin Complex; WB – Wilkes Basin; PSH – Porpoise Subglacial Highlands. To the right: Velocity structure of the ice drainage system of Antarctica (modified from Rignot et al., 2011). Black lines show the boundaries between the major ice basins.

3.2. Data and Methods

754 km of high vertical resolution (up to 3 m) multichannel seismic data were acquired on board of *RVIB Nathaniel B. Palmer* using a 75 m long, 24-channel streamer and paired 45 cubic inch Generator-Injector (GI) guns. The guns were towed at the depth of 2.5-3m and fired every 5 s resulting in a nominal ~12.5 m interval. The source frequency was within the range of 20-300 Hz. The seismic data set includes several dip- and strike-oriented profiles that extend across the shelf acquired opportunistically as ice cover and absence of protected species within the safety zones permitted (Fig. 3.2). Two-way travel time seismic profiles were used for the seismic stratigraphic interpretation. Data processing flow included trace regularization, bandpass and f/k filtering, spherical

divergence correction, muting, automatic gain control, normal moveout correction, stacking, water-bottom muting, and finite-difference time domain migration. The seismic grid was used to create isopach maps and to analyze seismic facies. Cross-correlation between seismic profiles was performed in DecisionSpace Software.

In addition, grid of high-resolution multibeam seafloor bathymetry data was used to complement seismic stratigraphic interpretation and infer the most recent history of glaciation and sedimentation in the study area. Two cores were used in this study to provide chronological control on the ages of the strata identified from seismic interpretation.

3.3. Background

3.3.1 Geological background

The rifted continental margin comprising Wilkes Land (~110°–130° E) was formed as a result of breakup and two-stage extension of East Antarctica and Australia, started in Late Cretaceous through the final separation and subsequent opening of Tasmanian gateway in the late Eocene *[Lawver and Gahagan, 2003; Close et al., 2010]*. In the Wilkes Land, basement of continental Australo-Antarctic crust belongs to Mesoproterozoic Mawson craton, which is overlain by two extensive, low-lying subglacial basins that mirror underlying tectonic architecture *[Donda et al., 2008; Aitken et al., 2014]*. Due to remoteness of the area, only few outcrops have been sampled. The closest outcrop is located on Windmill Islands about 1000 km to the west from the TG (Fig. 3.2) and shows the presence of Mesoproterozoic gneisses *[Zhang et al., 2012]*. Thus, major inferences about the geology of this poorly understood region have been made using integrated geophysical approach as well as the examination of pre- and syn-rift sediments of the conjugate South Australian margin *[Close et al., 2007]*.

Westernmost part of Wilkes Land includes the deep, lying more than 1 km below the sea level, Aurora Basin Complex, which in turn consists of the Aurora, Vincennes, and recently discovered Sabrina subglacial basins (ASB, VCB, SSB)(Fig. 3.2) *[Donda et al., 2008; Young et al., 2011; Aitken et al., 2014]*. ABC is bounded from neighboring Wilkes Basin by north-south oriented region of rough, rugged Porpoise Subglacial Highlands *[Drewry, 1978; Siegert et al., 2005; Donda et al., 2008]*. Geophysical studies

indicate that ABC is characterized by thick (up to 5 km) sedimentary cover and smooth topography, bounded by regional highlands that are deeply incised by wide (up to 50 km) valleys of glacial origin and channels emanating from these valleys towards the modern margin *[Siegert et al., 2005; Young et al., 2011; Aitken et al., 2014]*.

3.3.2. Glaciological background

Regional tectonic setting determines large-scale subglacial topography, which, in turn, controls the thickness of ice and major drainage pathways within ABC *[Young et al., 2011; Aitken et al., 2014]*. At the lowest point of the ASB, the bedrock is more than 1500 m below the sea level and the ice is over 4500 m thick *[Wright et al., 2012]*. ABC mass discharge is dominated by fast-flowing, marine terminating MUIS and TG (Fig. 3.1) *[Rignot et al., 2011; Wright et al., 2012]*. Unnamed highlands located eastward of the MUIS (122°–128° E) (Fig. 3.2) are recognizable on the regional BEDMAP2 grid *[Fretwell et al., 2013]*. These highlands host parts of the ice sheet that currently demonstrate significantly slower velocities when compared to neighboring TG and MUIS *[Bamber et al., 2000; Rignot et al., 2008]*. Currently, TG and MUIS show negative mass balance, whereas glaciers descending from the highlands don't show evidence of thinning or retreat *[Zwally et al., 2005; Pritchard et al., 2009; Rignot et al., 2013]*.

Well-distributed system of extensive subglacial water conduits exists beneath the ice in ASB and SSB, suggesting a hydrological link between abundant subglacial lakes of ASB and SSB and the termini of their outlets *[Wright et al., 2012]*. The ice sheet is currently warm based across WSB and ASB, whereas SSB and areas dominated by rugged highlands, such as Porpoise Subglacial Highlands, host cold-base ice *[Siegert et al., 2005; Wright et al., 2012]*.

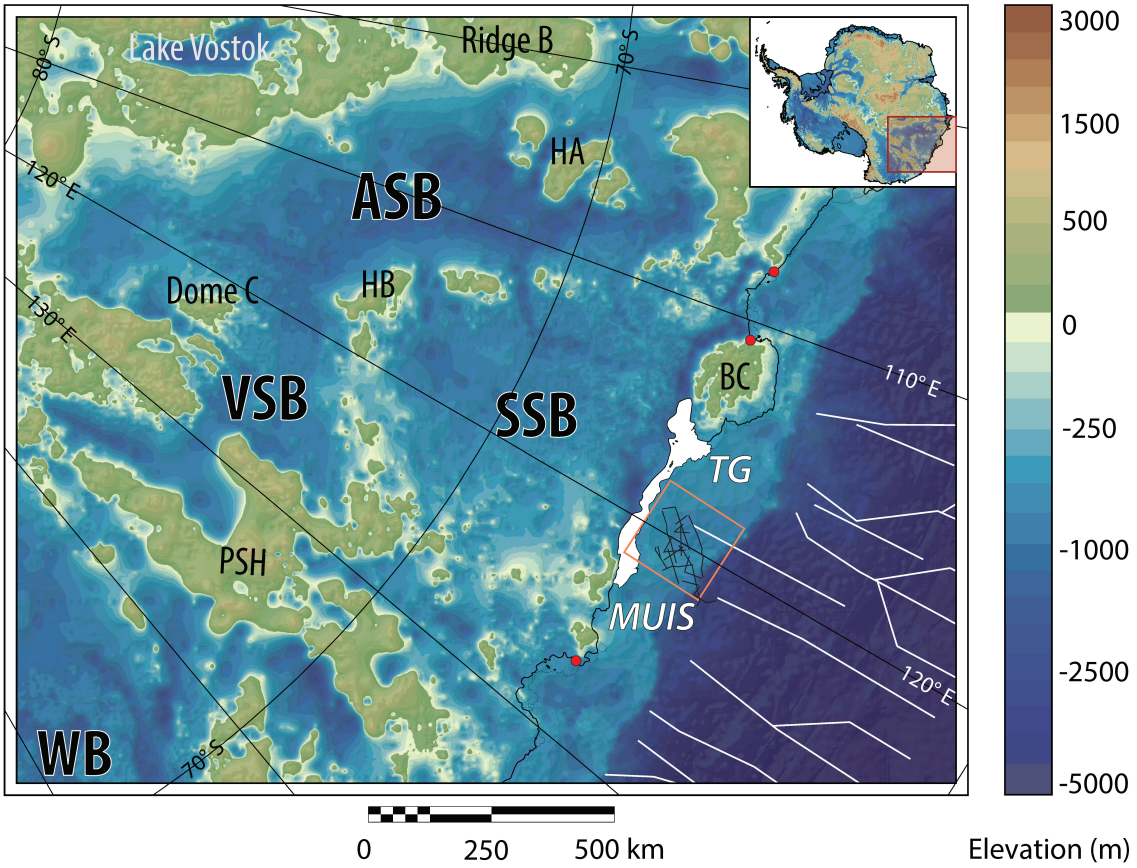

Fig. 3.2. Aurora Basin Complex (ABC). Sub-basins include Aurora Subglacial Basin (ASB), Sabrina Subglacial Basin (SBB) and Vincennes Subglacial Basin (VSB). Porpoise Subglacial Highlands (PSH) are to the east of ABC. Study area is shown with orange box with black lines demonstrating the location of the seismic profiles. Red dots show the locations of outcrops most proximal to the study area *[from Aitken et al.,2014]*. Map is based on BEDMAP2 data *[Fretwell et al., 2013]*.

3.3.3 Sabrina Coast margin physiography and Cenozoic sedimentation

Whereas rifting shaped initial architecture of the continental margin adjacent to the Sabrina Coast, for million years that followed Cenozoic glaciation the modern margin physiography has been sculpted by ice-sheet related processes. Although no high-resolution bathymetric studies have been done on the shelf until Sabrina Coast expedition, previous low-resolution bathymetric maps suggest an irregular, foredeepened and overdeepened shelf occupied by morphologic features that resemble glacial troughs, suggesting effects of ice loading and glacial erosion, phenomena that are commonly observed at Antarctic margins *[e.g., Anderson et al., 1999; Bart ad Iwai, 2012]*. The shelf

width increases westward from 130 km at the eastern tip of the MUIS terminus to 180 km at the terminus of TG, to the west of which it narrows down dramatically towards the Budd Coast, becoming only 40 km wide. Slope gradients show variation from about 2° across eastern part of MUIS (~123° E) to 9° between MUIS and TG back to 1° in the part of the margin adjacent to the Budd Coast. The slope is dominated by a few broad, downslope-diverging fans and valleys, including the prominent Aurora Channel located on the lower slope (~120°E) *[Close et al., 2007; Donda et al., 2008]*.

All to-date studies of Sabrina Coast margin sedimentation represented parts of regional Wilkes Land seismic stratigraphic studies *[e.g., Eittreim, 1987; Colwell et al., 2006; O'Brien et al., 2006; Close et al., 2007; Donda, 2008; Close et al., 2010]* with only one regional seismic profile capturing a fraction of the shelf, area that is critical for understanding ice-contact processes and grasping the full context of glacial sedimentation at the margin. The regional study of slope and continental rise sedimentation of Wilkes Land revealed prominent, more than 10 km thick Budd Coast Basin (BCB) offshore the TG terminus, which was interpreted to reflect the long lasting role of TG feeding the BCB by providing the focused sediment delivery to the slope *[O'Brien et al., 2006; Close et al., 2007]*. Slope portion of BCB is recognizable on the bathymetry data as distinctive convex shaped, bulging feature that resembles seafloor expression of shelf progradation typically resulting from the development of large trough mouth fans (TMF) *[e.g., Vorren et al., 1997; O'Grady and Syvitsky, 2002; O'Cofaigh et al., 2003; Stokes et al., 2006]*.

3.3.4 Antarctic Cenozoic glaciation

Several major stages in the development of Antarctic Ice Sheet have been recognized based on high-resolution deep-sea marine oxygen isotopes. Ice sheets built up on Antarctica approximately 34 million years ago as a result of Oi-1 event *[e.g., Zachos et al., 2001]*. Throughout the Oligocene, glaciation has likely waxed and waned *[Naish et al., 2001]*. The late Oligocene and early Miocene periods, have generally been viewed as times of mainly ice-free conditions, although there is evidence of several glacial expansion episodes *[e.g., Cooper et al., 1991; Zachos et al 1997; Naish et al., 2001]*. Such conditions lasted until Mid Miocene, when the global climate established gradual cooling trend *[e.g., Zachos et al., 1992, 2001]*. Although it is known that AIS has undergone considerable fluctuations since the early Eocene-late Oligocene, the nature of

these fluctuations, particularly during the initiation and growth stages of early AIS development remains unclear *[Siegert and Florindo, 2008]*.

Numerical models that predict the feedbacks between the dynamics of AIS and oscillations of global climate have to be constrained by records of glaciations that have occurred in the past. The history of AIS development has been inferred largely from ice cores, drilling data, sedimentary facies, and seismic images as well as geological evidence from rocks and fossils from the Antarctic continent *[Francis et al., 2008]*. Of these methods, marine seismic studies are particularly important because they can help elucidate record of ice-seafloor interactions preserved as geomorphological features imprinted within sedimentary architecture of the margin thus providing an opportunity to potentially document important climatic transitions such as the initiation and growth of the early AIS.

3.4. Bathymetry

3.4.1. Observations

Continental shelf off MUIS demonstrates a considerable range of the seafloor depths, from 200 m in the eastern and southern parts of the study area to over 1000 m in the north and west (Fig. 3.3). Swath-bathymetric data reveal several types of landform assemblages of different scales present on the inner and mid-shelf. The largest-scale landform is a deep (up to 700 m) depression trending predominantly in the north-west direction. The exact width and length of the depression are unclear due to the limited data coverage. Areas outside of the depression show much shallower seafloor depths and are dominated by different landform assemblages.

Within the extent of the depression three smaller-scale features dominate the seafloor morphology. The first set of features represents streamlined lineations elongated in the direction of the large-scale depression and occurs at the southwest part of the study area (Fig. 3.3D). They are frequently spaced (~100-300 m), up to 15 m high and reach lengths of up to 20 km. Second type of landforms are found in the eastern part of the depression and represent drop-like shaped lineations with wider ends directing towards the coastline found in the eastern part of the depression (Fig. 3.3B). These features are up to 400 km wide, 40 m high and 3 km long. The third landforms assemblage is represented by wedge-shape, convex features that dominate the northern part of the depression (Fig.

3.3A). Two wedges found within the depression have complex shapes, are 40-km wide, up to ~100 m high, and are oriented obliquely (about 60 deg) to the direction of the lineations. Finally, inner elevated part of the shelf adjacent to the depression is dominated by a relatively flat surface that shows extensive, irregular crack-like morphology (Fig. 3.3C), incised in different directions by up to 100 m deep, 1 km wide linear depressions.

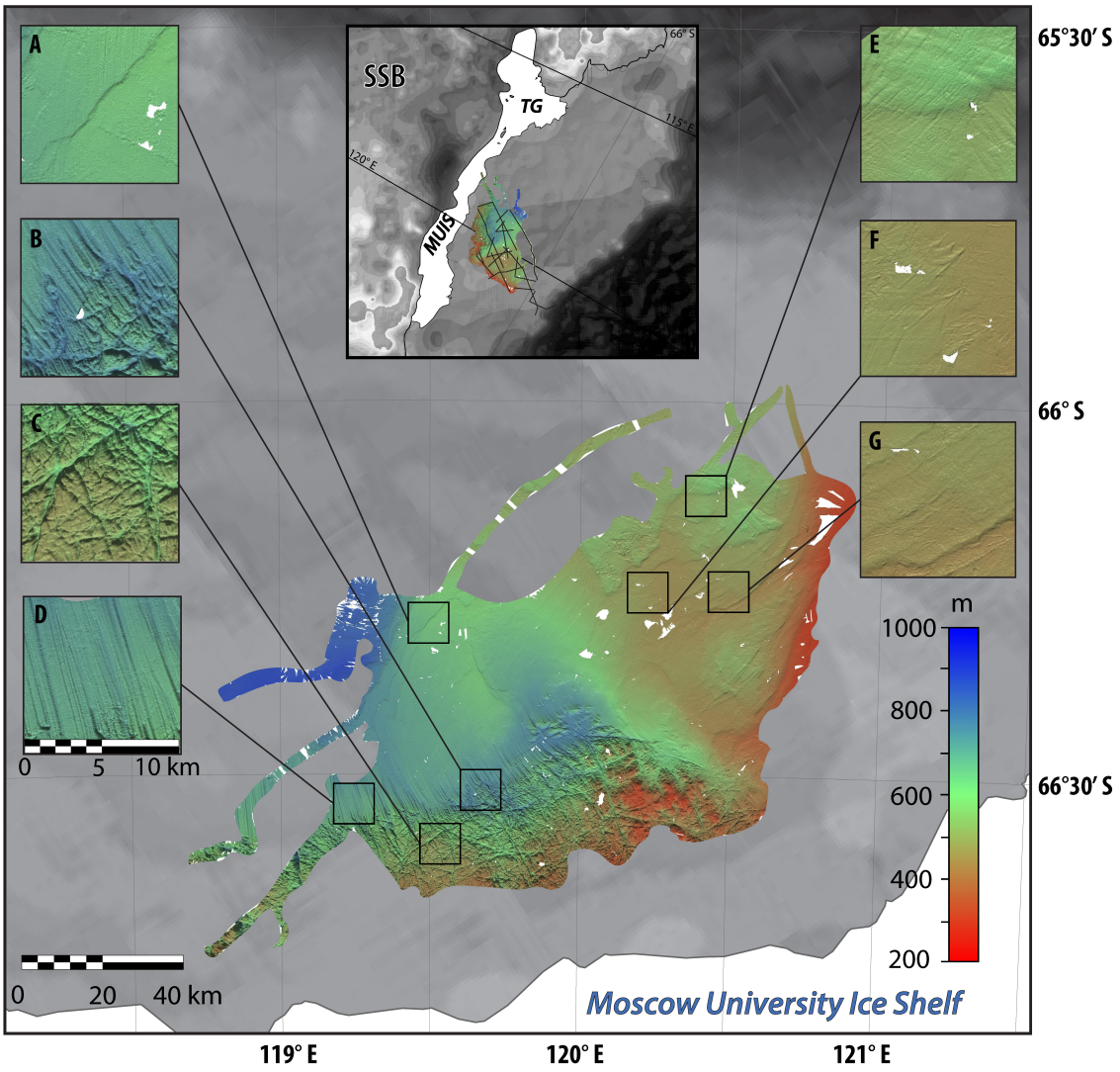

Fig. 3.3. High-resolution swath-bathymetry data used in this study. Box in the upper part of shows the regional context of data coverage, black lines represent locations of seismic profiles. Small boxes show magnified seafloor landform assemblages: (A) grounding zone wedges (GSWs); (B) drumlins; (C) ice-sculpted bedrock; (D) mega-scale glacial lineations (MSGLs); (E) recessional morainal ridges; (F) iceberg ploughmarks and (G) large-scale retreat moraines.

Outside of the depression, three major types of landforms are present. The first represents slightly concave, wedge-shape features that trend parallel to the shelf edge (Fig. 3.3G). Six wedges spaced at about 10 km apart are up to 30 km wide and dominate the eastern part of the investigated inner shelf. The second type of landforms has been found in the northern part of the area and represents sets of smaller transverse ridges (Fig. 3.3E). These ridges are frequently spaced (from ~200 m) and have amplitudes less than 20 m. Finally, irregular furrows that crosscut one another are present (Fig. 3.3F). These features are up to 10 kilometers long, ~150 m wide, and ~15 m deep.

3.4.2. Interpretation

The large-scale, deep and wide depression is interpreted as cross-shelf glacial Reynold's Trough (RT). Such troughs have been widely recognized in high-latitude margins from both hemispheres and are interpreted to result from the excavation produced by fast-flowing ice streams and outlet glaciers that possess focused ice flux sufficient to erode and transport significant amounts of sediments to the shelf break *[e.g., Carlson, 1989; Vorren et al., 1998; Shipp et al., 1999; Dowdeswell and Elverhøi, 2002; Ottesen et al., 2005, 2007; Ottesen and Dowdeswell, 2009; Batchelor et al., 2014]*. This interpretation provides evidence that at least during last full-glacial period at least one fast flowing ice stream drained the ABC. The location and direction of the trough suggest that this ice stream emanated from modern MUIS and flowed in the southeastern direction from the modern shoreline. Within the trough, its proximal part adjacent to the exposed bedrock is eroded deeper than the surface farther offshore, which is likely to represent consequence of overdeepening, a phenomenon common for Antarctic continental margins *[e.g., Bart and Iwai, 2012]*.

Long, northwesterly oriented lineations found within the trough are interpreted as Mega-Scale Glacial Lineations (MGSLs). These lineations are common features found within the cross-shelf troughs and represent the result of fast flowing ice advancing across the shelf and deforming soft sediment at its base *[e.g., Clark, 1993; Anderson et al., 2001; Ó Cofaigh et al., 2005; Dowdeswell et al., 2004; Dowdeswell et al., 2007]*. Shorter drop-like features are interpreted as drumlins and represent another morphological feature diagnostic of fast flowing ice advancing across the shelf that typically occur at the transition between exposed bedrock and sedimentary strata that

covers the outer shelf *[e.g., Anderson et al., 2001; Wellner et al., 2001; Stokes, 2001; Sugden et al., 2006]*. Dimensions and geometry of the wedge-shaped, convex features are similar to the grounding-zone wedges (GZWs) that form at the terminus of an ice stream during a long still-stand in the phase of retreat *[e.g., O'Brien et al., 1999; Ottesen and Dowdeswell, 2009; Dowdeswell and Fugelli, 2012]*. The presence of two of these wedges implies at least two, hundreds of years long halts in ice stream retreat. In addition, the obliquity of the GZW fronts relative to the orientation of MSGLs implies that during the last interglacial, the ice stream narrowed and shifted laterally towards the eastern flank of the trough with the terminus oriented obliquely to the direction of the flow. Finally, the irregular cross-cut pattern of inner shelf suggests that it is composed of exposed bedrock, heavily incised by the ice stream. Such ice-sculpted bedrock is widely interpreted in both hemispheres *[e.g., Anderson et al., 2001; Ottesen and Dowdeswell, 2009; Livingstone et al., 2012; Batchelor et al., 2014]*. This interpretation is also in agreement with studies by Aitken et al., *(2014)*, who suggested that inner shelf adjacent to the Sabrina Coast is composed of Proterozoic granitic intrusions.

The shallower eastern part of the study area represents eastern bank of the trough. Six regularly spaced, wedge-shaped concave features have dimensions similar to GZWs observed within the trough. These features are interpreted to represent large retreat moraines formed during periods of stillstand retreat of a grounded ice margin *[Ottessen and Dowdeswell, 2009]*. Smaller amplitude, densely spaced transverse ridges represent series of small push moraines that likely resulted from a minor readvance of a glacier terminus following general retreat trend *[e.g., Boulton, 1986; Shipp et al., 2002; Ottesen et al., 2008]*. These landforms are generally produced by grounded glaciers that are not fast flowing *[Dowdeswell et al., 2007]*. Finally, irregular identations found on the seafloor of the trough bank are interpreted as iceberg ploughmarks, formed by icebergs scouring the shallower shelf *[e.g., Anderson, 1999; Ó Cofaigh et al., 2002; Batchelor et al., 2014]*.

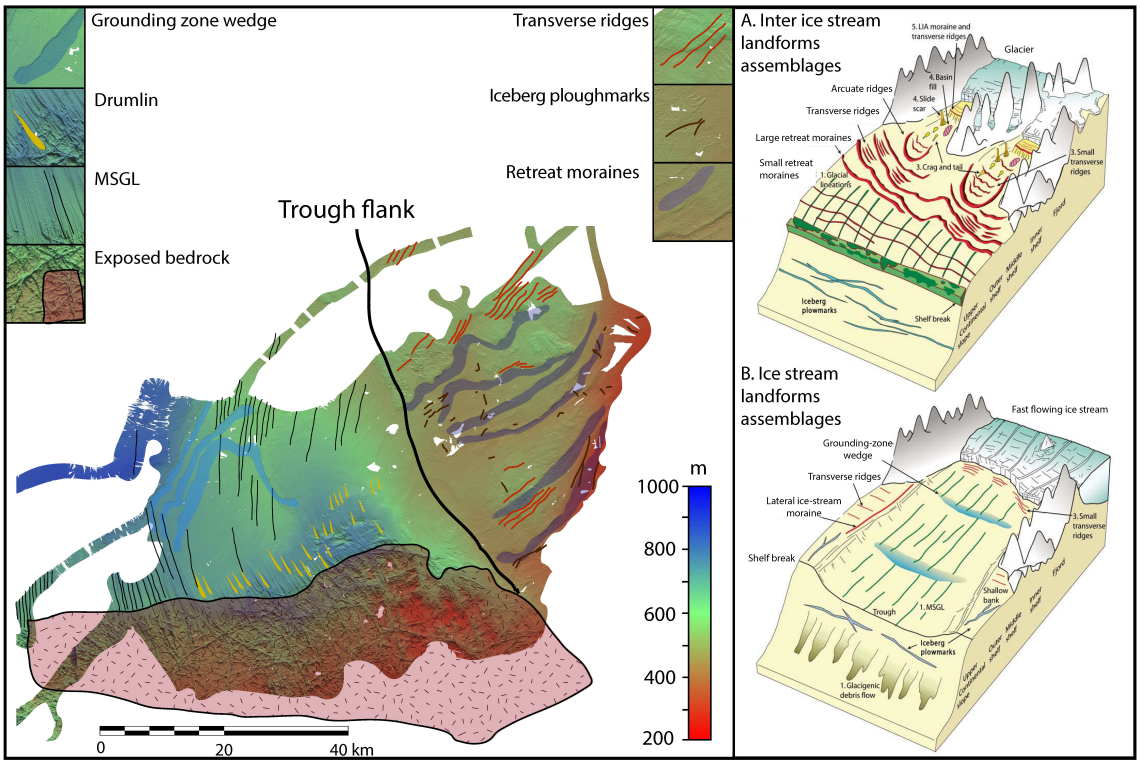

Fig. 3.4. To the left: Interpretation of landforms assemblages within the Reynold's Trough. To the right: Conceptual model of ice stream and inter-ice stream landform assemblages from Ottessen and Dowdeswell, (2009).

Assemblages of various landforms observed offshore MUIS provide evidence of grounded ice advance across the shelf, document the pattern of former ice flow and imply two principally different ice flow regimes during at least last glacial-interglacial. We observe three times more large moraines in the trough bank compared to the number of GZWs within the trough which implies either fewer stillstands of decadal or greater duration, or faster rates of ice retreat within the trough. In either case, this observation suggests different dynamics of ice retreat within and outside the trough. The trough exhibits features that are diagnostic of a fast flowing ice stream, whereas the shallower bank demonstrates landforms typically produced by slower flowing grounded ice. This interpretation is supported by the larger-scale geological and glaciological picture, which implies that thick ice volumes within the ASB and SSB, that serve as interior drainage basins for TG and MUIS, provide sufficient ice flux which are capable of producing fast flowing ice, compared to the highlands adjacent to the trough bank, which are unlikely to

host thick ice and represent relatively restricted catchment and, therefore, are likely not capable of providing fast-flowing ice streams *[Dowdeswell and Elverhøi, 2002]*.

3.5. Seismic stratigraphy

3.5.1 Seismic facies and morphological features

Based on the geometry and structure of internal reflections we differentiate five major seismic facies that dominate the composition of seismic sequences of the Sabrina Coast shelf. This classification is based on previous lithological and seismic investigations at high latitude margins *[e.g., Carlson et al., 1989; Anderson et al., 1992; Cai et al., 1997; Bart et al., 2000; Powell and Cooper, 2002; Dowdeswell et al., 2007; Batchelor et al., 2013]*. In order to be consistent with classifications of seismic facies outlined by previous workers, we adopt existing facies nomenclature from most recent seismic stratigraphic studies of Canadian Arctic *[Batchelor et al., 2013]*.

Facies S shows well-stratified character of seismic reflections with individual reflections being parallel or sub-parallel to each other (Fig. 3.5). Reflections within facies S vary from high to low amplitude. Facies C has transparent, internally chaotic to poorly stratified character of seismic reflections, and occurs either in a form of sheet-like deposits bounded by one or more high-amplitude parallel reflectors (C_s), or in a form of a wedge-shaped body (C_w). Facies H has hummocky, irregular, channelized, mainly chaotic structure of internal reflections with occasional mound-shaped high-amplitude reflectors (Fig. 3.5). Facies N contains acoustically transparent reflections and a highly irregular, rugged high-amplitude capping reflection.

We identify four key morphological features based on their geometry, facies content and relationships to bounding strata. Progradational wedges with dipping internal reflectors of high- to low-amplitude occur between high-amplitude reflectors. Deep (about 150 ms TWT) and wide (up to 1500 m) channels truncate underlying reflectors and have chaotic internal character with occasional mounded, high-amplitude reflections. Indentations of smaller dimensions (about 700 m wide and up to 40 ms TWT deep) but similar internal configuration occur within the older sequences. Up to 100 ms TWT thick, and up to 25 km wide wedges with chaotic, low- to high-amplitude internal acoustic

character are bounded by very pronounced, high-amplitude single reflectors (Fig. 5).

Seismic facies	Example	Description	Seismic feature	Description
S	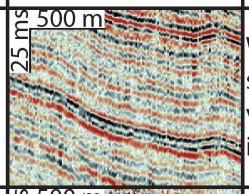	Well-stratified, parallel to sub-parallel reflections, variable acoustic impedance.	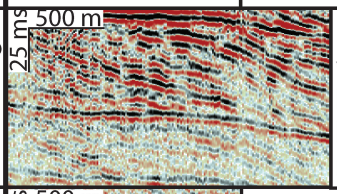	Progradational wedge-shaped bounded by horizontal reflections.
H	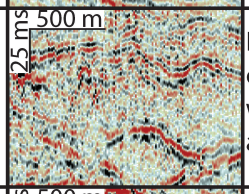	Hummocky, internally chaotic, channelized, with individual high-amplitude reflections.	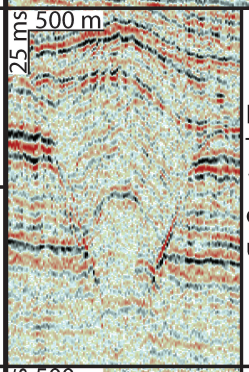	Deep (up to 150 ms TWT), wide (up to 1150 m) incised channels truncating underlying reflectors.
C_w	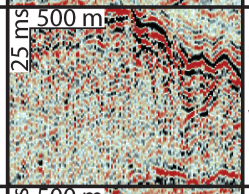	Chaotic, low-amplitude internal reflections, wedge-like external configuration.		
C_s	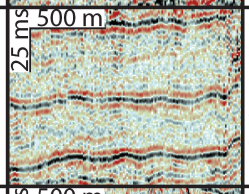	Low-amplitude internal reflections, sheet-like external configuration.	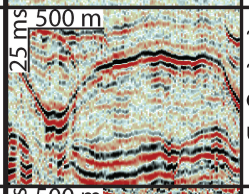	~50 ms TWT deep, ~750 m wide incised channels truncating underlying reflectors.
N	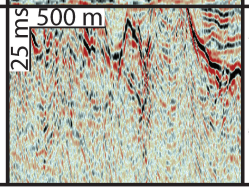	Acoustically impenetrable, with high-amplitude exernal reflections of rugged configuration.	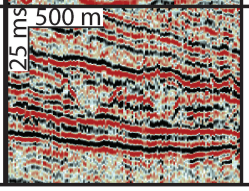	~25 ms TWT deep, ~250 m wide indentations. Truncate underlying reflectors.

Fig. 3.5. Seismic facies and morphological features found within Sabrina Coast shelf seismic stratigraphic record.

3.5.2 Large-scale shelf sequences composition: general overview

Seismic reflection data reveal that the inner shelf is dominated by acoustically impenetrable facies N that deepen towards the shelf break (Fig. 3.6). The chaotic character of seismic data together with the rugged shape of the capping reflector suggest that facies N represents the exposed ice-scuplted bedrock, which is in agreement with swath-bathymetry data interpretation. The sediments overlying the bedrock were divided into 3 megasequences (MSs) (Fig. 3.6), based on the major transitions between dominant seismic facies and the presence of regionally widespread erosional surfaces. The goal of this study was to give detailed description and perform analysis of MS II. A general overview and description of all MSs is provided below.

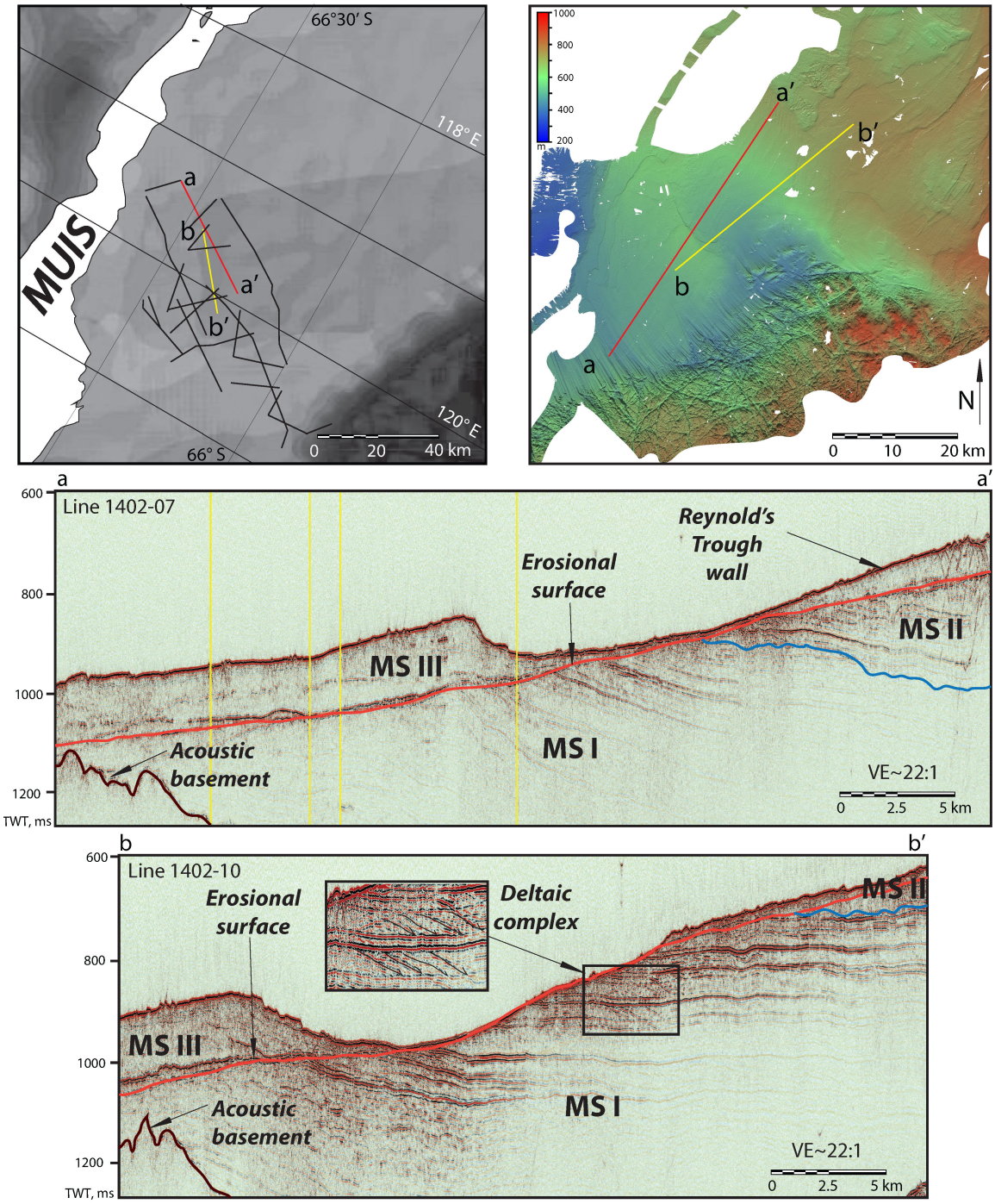

Fig. 3.6. Large-scale seismic stratigraphic record of SC inner shelf. Brown rugged surface represents acoustic basement, which is the base of MSI. Blue undulating surface is the base of MSII, which is separated from MS III by the regional erosional unconformity shown in red.

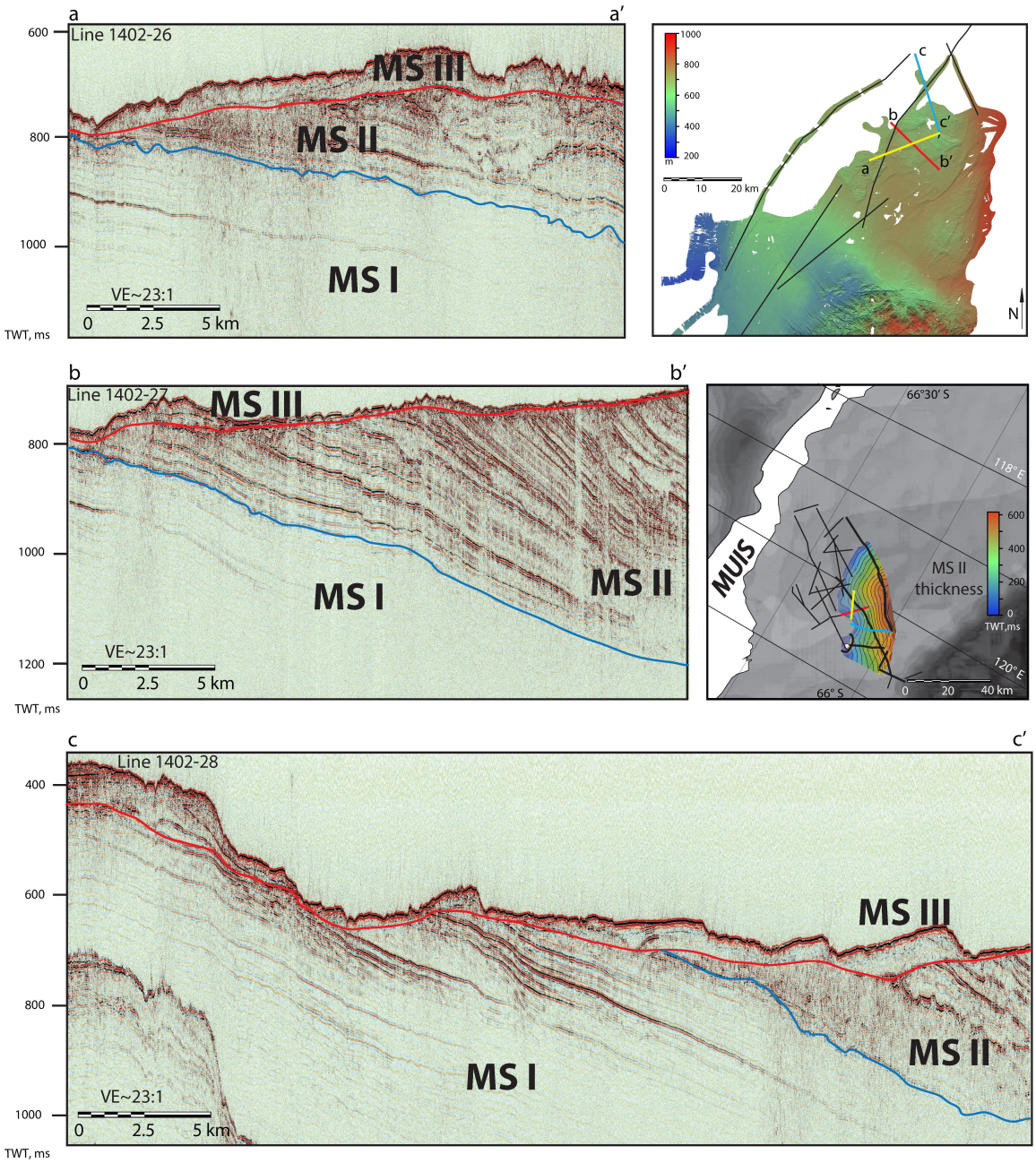

Fig. 3.7. Seismic stratigraphic record of SC mid-shelf. Blue undulating surface is the base of MSII, which is separated from MS III by the regional erosional unconformity (RES) shown in red. The isopach of MSII is shown on the regional map (top right).

Megasequence I (MSI) is composed of a thick series of stratified, mostly low-amplitude, parallel reflectors of facies S that overlie rugged surface of facies N and demonstrate gentle dip and thickening towards the shelf break (Fig. 3.6). The upper part of MSI is comprised of a series of progradational wedges bounded by high-amplitude reflectors. Megasequence II (MSII) is composed of several sequences that are dominated

by facies H, C and S. Its base is a deep, undulating, irregularly channelized surface truncating reflections within the upper part of MS I. Within the study area, MSII reaches depths of up to 600 ms TWT (Fig. 3.7). Megasequence III (MSIII) is composed of irregularly placed, stacked wedges containing facies C_w, lying on top of the prominent regional erosional surface (RES) that truncates topsets of dipping strata within MS II.

We have interpreted eight major units that comprise MSII within the extent of available data. Each unit was distinguished based on two main criteria: (1) presence of an erosional surface truncating underlying strata at its base and (2) change in the predominant seismic facies content.

3.5.3 Units 1 and 2

3.5.3.1. Description

Units 1 and 2 show significant thinning from ~200 m to ~100 m in the southwest direction and each include 2 sub-units bounded by 2 major undulating, channelized erosional surfaces (Figs. 3.8 and 3.9). The basal reflection truncates strata below, showing highly irregular morphology with elevation amplitudes of up to ~100 m and widths of individual undulations of up to ~7 km. The base of Unit 1 (h1) exhibits a gentle dip (~1°) towards the shelf break following the dip of the strata below. Bottom part of Unit1 is composed of facies H, which demonstrates thickness variability between two cross-sectional seismic lines 1402-29 and 1402-21 (Fig. 3.8). Thick (up to ~100 m) layers of facies S with presence of few high-amplitude reflectors overlie the hummocky surface of facies H. Around 100 m thick and 10 km wide wedge of facies C_w is bounded from neighboring layers of facies S by two incised channels.

Unit 2 is composed entirely of facies H and shows evidence of at least three undulating erosional surfaces (h2, h2.2 and h3) identified on seismic profile 29. The most prominent erosional surface is found at the base of Unit 2, with elevation amplitudes of up to ~120 m and variable morphology. This variability includes the presence of two symmetric, deeply incised channels with widths of up to 1150 m and depths of ~110 m that are found in the eastern part of profile 29, whereas western part is dominated by asymmetric, wide channels of approximately the same depths.

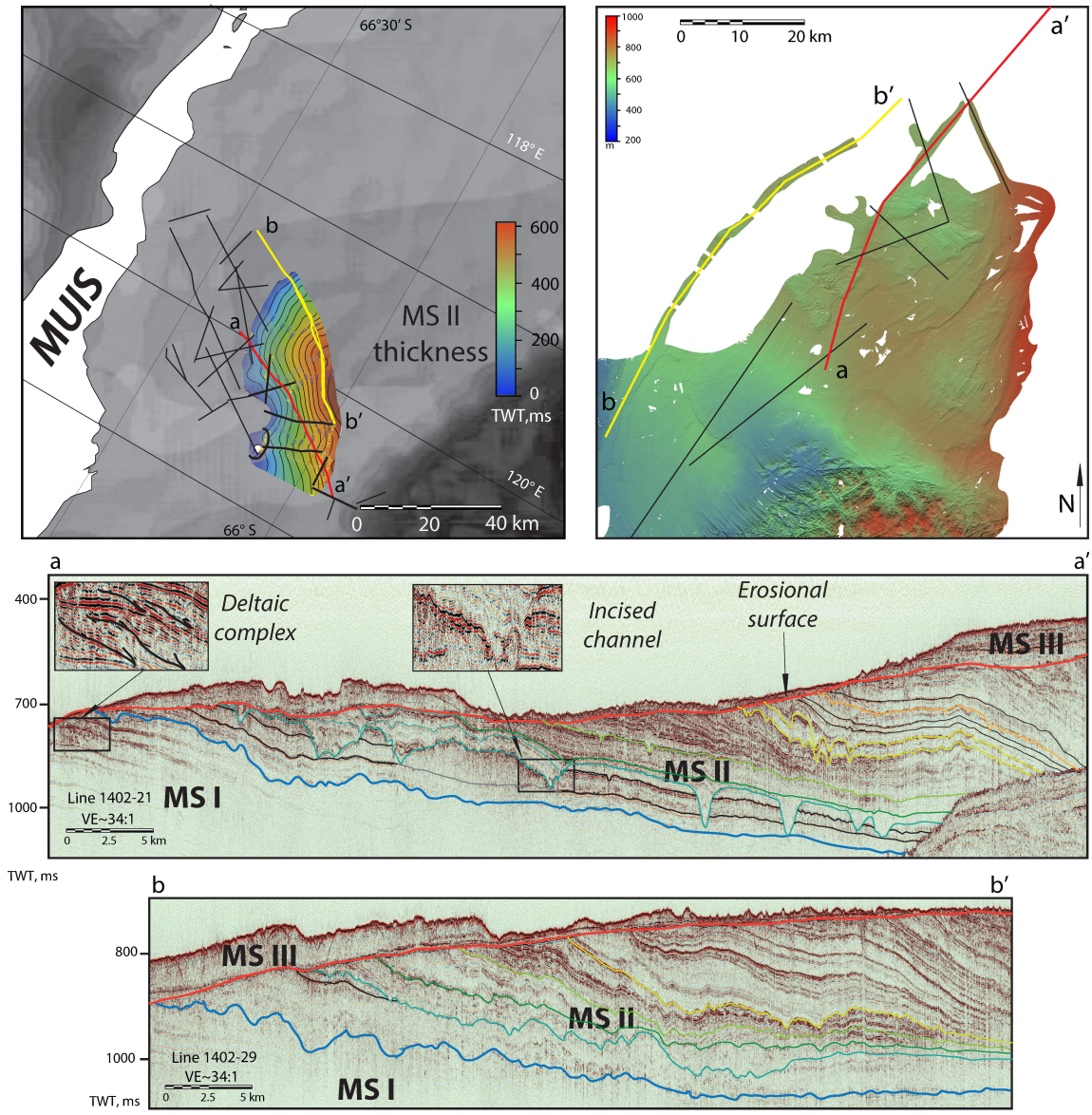

Fig. 3.8. Seismic stratigraphic record of SC shelf showing the most complete composition of MSII from two strike oriented seismic profiles.

3.5.3.2. Interpretation

Erosional surfaces that show configurations similar to the irregular, undulating basal surface of Unit 1 (h1) are not a common finding among seismic stratigraphic studies from Antarctic margins *[e.g., Erohina et al., 2004]*. Seismic data from ODP Sites 742 and 1166, Prydz Bay, have revealed broadly undulating subsurface geometry, with an internal weak hummocky acoustic character and the presence of deformed sands *[Erohina et al., 2004]*. Hambrey et al., *[1991]* suggested that the same deformed sands

unit at the bottom of neighboring Site 742 resulted from glaciotectonic deformation. Erohina et al., *[2004]* proposed an alternative interpretation suggesting that the deformed sands resulted from activity of an outwash system from upstream glaciers within the Lambert Graben. However, scanning electron microscopic (SEM) microtextural analysis of quartz grain surfaces recovered from the base of undulated surface at Site 1166, revealed relative abundance of angular grains (30‑50%) and the presence of grains with features that only develop in a subglacial environment, supporting the primary hypothesis by Hambrey et al., *(1991) [Strand et al., 2003]*.

Thus, limited analogs from integrated seismic and lithostratigraphic studies from Antarctic margins do not provide unambiguous constraints on the genesis of these distinctive morphological features, although favor a glacial rather than fluvial origin. The high amplitudes of elevation changes within the undulating surface also argue for it to represent the base of the channel system developed by significant fluxes of meltwater transferred from the interior parts of ice sheet to the margin *[e.g., Lowe and Anderson, 2003; Denton and Sugden, 2005; Smith et al., 2009]*. One of the main arguments for this interpretation has been that undulating thalwegs incised into such depths are unlikely to be formed by fluvial incisions caused by lowstands *[Huuse et al., 2000; van der Vegt et al., 2012]*. Thus, we interpret the undulating, irregular base of Unit 1 as the signature of first grounded, polythermal EAIS on the shelf off Sabrina Coast.

The thick cover of stratified facies S on top of the undulating surface suggests that ice retreated after the initial polythermal expansion followed by significantly long period of ice-distal to open-marine conditions, which resulted in deposition of well-sorted, stratified sediment. Such interpretation of facies S is consistent with lithological and seismic stratigraphic studies from both hemispheres *[e.g., Cai et al., 1997; Batchelor et al., 2013; Dowdeswell et al., 2014]*. Within facies S, the individual high-amplitude reflector with traces of shallow channelization might represent a short period of ice advance closer to the shelf with subsequent development of shallow pro-glacial fluvial complexes. However, there is no seismic evidence of erosion associated with ice advancing across the shelf until the development of another series of deeply incised channel system comprising unit 2.

The most striking features within the undulating surface of h2 (basal surface of Unit 2) are two symmetric channels incised into the Unit 1 (Figs. 3.9 and 3.10). Morphometrically, these channels are very similar to subglacial tunnel valleys widely documented by studies from both hemispheres *[e.g., O'Cofaigh, 1996; Huuse et al., 2000; Denton and Sugden, 2005; Lonergan et al., 2006; Kristensen et al., 2007; Stewart and Lonergan, 2011]*. The asymmetric, undulating configuration of the channels found to the west of these two tunnel valleys suggests that the channel system was organized into a complex, anastomosing pattern, which is very common for subglacial meltwater systems across the globe *[e.g., Denton and Sugden, 2005; Lonergan et al., 2006; Smith et al., 2009]*. This, in turn, provides additional argument in favor for the undulating base of Unit 1 (h1) to represent the signature of earlier tunnel valley system as well. However, there are no symmetric, deep channels found within the Unit 1, possibly due to incomplete record caused by prominent erosion of the western part of the stratigraphic record.

Unit 2 is composed entirely of facies H and bounded by channelized surfaces, which likely reflects a series of consecutive advances of polythermal ice across the shelf. Absence of facies S within the record of this unit argues against erosional surfaces to represent separate glaciations unless any evidence of ice distal deposition was completely eroded by subsequent glacial advance. Rather, the ice sheet front has oscillated across the shelf during one larger scale glacial event without retreat far inland and deposition of interbedded, stratified sediment.

The nature of the very thick, isolated wedge of chaotic facies Cw remains uncertain. The acoustic character together with wedged shape suggests that it represents a moraine deposited after glacial retreat *[e.g., Cai et al., 1997]*. However, this interpretation requires erosional surface to occur at its base. The chaotic inner reflections of the wedge do not allow for identification of such reflector, allowing for several possible scenarios of the wedge origin and the timing of its formation to occur between incision related to h1 and h2.

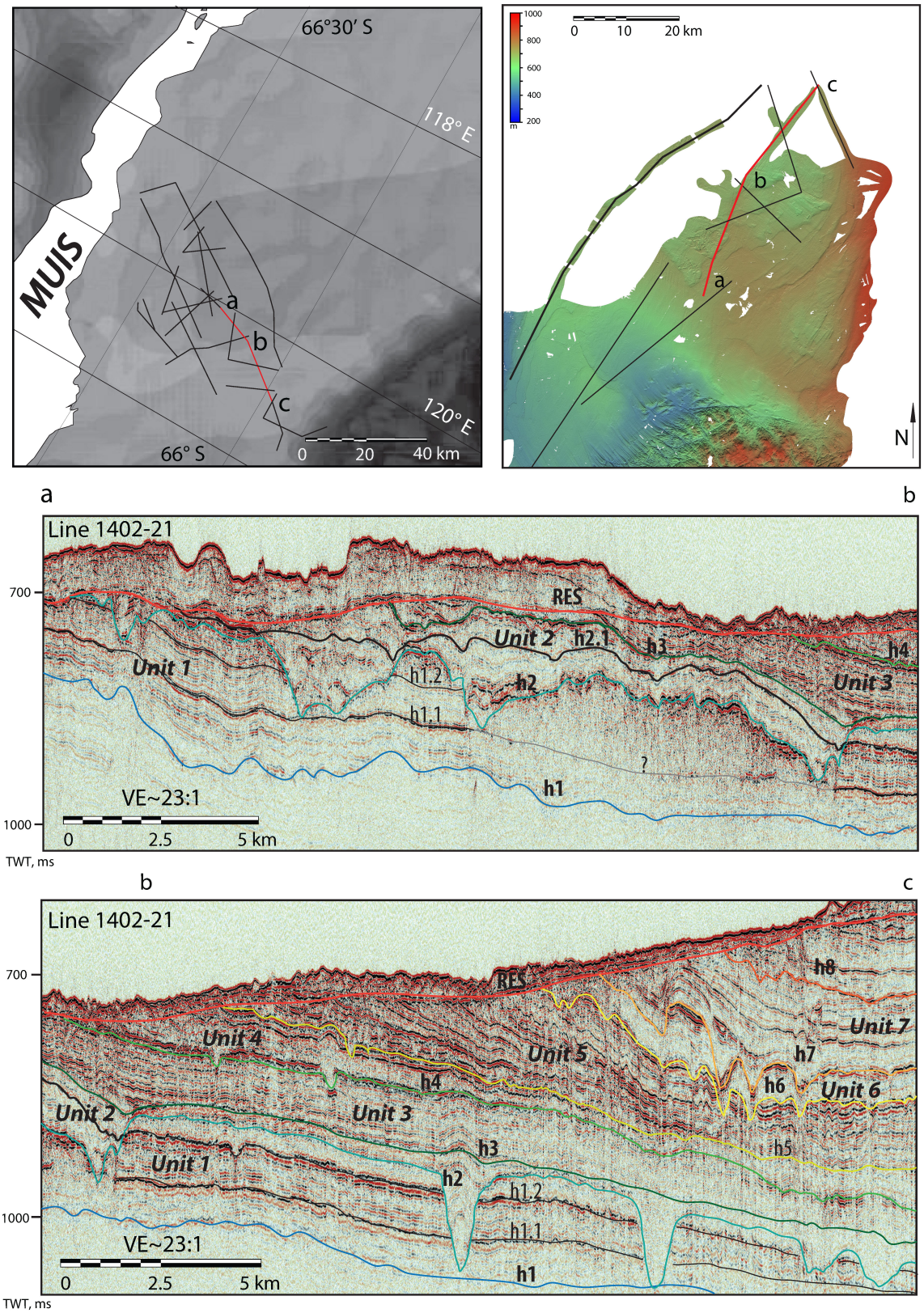

Fig. 3.9. Facies composition and individual erosional surfaces interpreted within MSII from seismic line NBP1402-21.

The observed overall thinning of Units 1 and 2 towards the eastern part of the study area may be caused by: (a) deeper erosion of the h1 in the western part of the sequence and (b) thicker parts of Units 1 and 2 deposited within the western part of the sequence. Assuming the profiles 29 and 21 represent cross sections, this observation implies that eastern part of the study area experienced more both erosion and deposition and hence, the glacial processes of greater intensity. Therefore, the configuration of ice front of early EAIS was likely to be non-uniform across the SC margin.

3.5.4 Units 3-4-5

3.5.4.1. Description

Unit 3 is composed entirely of facies S, which shows acoustic impedance attenuation towards the eastern part of the section. In the bottom part of the sequence, individual reflectors are onlapping the h3 (Fig. 3.9). Unit 3 shows thinning in the west-east direction. The stratified character of unit 3 is interrupted by erosional surface h4 that represents the base of Unit 4. Surface h4 shows indentations of ~30 m deep. In the plane of profile 21, Unit 4 represents a thin package of facies C that thickens westward and is overlain by a thin drape of high-amplitude facies S. On profile 21, Unit 5 is up to ~ 150 m thick and is dominated by high-amplitude facies S with occurrence of small (~15 m) indentations and thin layers of transparent facies C.

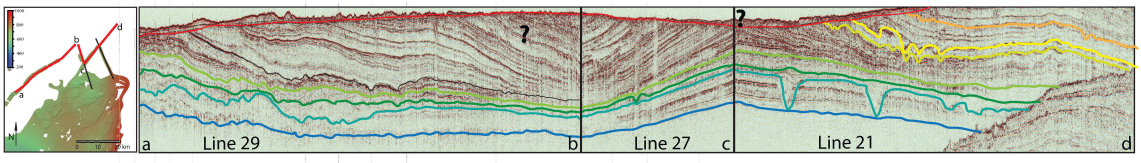

Fig. 10. Cross-correlation of surfaces above h5 between two cross-sectional lines 1402-21 and 1402-29 is problematic due to regional erosion expressed by surface RES.

Due to the prominent erosional surface RES, it is problematic to reliably correlate and confidently claim the extent of units above Unit 5 across two profiles 21 and 29 (Fig. 3.10). However, our interpretations suggest that Unit 5 thickens to the west and exhibits greater detail of facies composition. On the profile 29, it is up to ~200 m thick and is composed of mainly facies S with occurrence of an ~50 m thick wedge-shaped body composed of facies C (Fig. 3.12). Acoustically, facies S within Unit 5 varies

significantly, from thick layers composed of transparent, stratified reflections to individual thin series of high-amplitude, draping reflections.

3.5.4.2. Interpretation

The acoustic character of Unit 3 and absence of erosional surfaces suggests that this unit was formed in ice-distal to open-marine environment. The change in acoustic impedance contrast throughout the section most likely reflects the effects of spherical divergence and energy attenuation rather than lithological differences within the strata. Facies content of Unit 4 and erosional character of its base imply that it reflects a single glacial advance. Given lateral unit thickness variability and pinch-outs observed in the eastern part of the study area, it is possible that Unit 4 may have been even thicker in the western part of SC shelf.

The origin of Unit 5 is more likely to represent deposition mostly during ice-distal conditions with possible minor glacial advance evident from the thick wedge of chaotic facies bounded by thick series of facies S. It is possible that there may have been more erosional events during the deposition of Unit 5, that could be found within the shelf stratigraphy to the west of the study area. Variations in acoustic impedance reflect changes in grain size and lithofacies, which in turn are likely controlled by the combination of changes in shoreline and glacial proximity *[Naish et al., 2001]*. Thus, the observed layers composed of low-amplitude, almost transparent facies S may reflect long periods of deposition with very minor changes in depositional environment and, as a consequence, no significant lithological contrast.

3.5.5 Units 6-7-8

3.5.5.1. Description

Upper part of Unit 5 is truncated by surface h6, that is dominated by indentations with amplitudes of up to ~40 m. H6 represents the base of relatively thin (~50 m) Unit 6, which is composed of facies C. Erosional, undulating surface h7 truncates the top of the Unit 5 and is morphologically similar to h6, showing slightly deeper incisions. Unit 7 overlies the h7 and is composed of an ~ 50 m thick layer of facies C in its bottom part. Upper part of Unit 7 comprises draping layers of low-amplitude facies S bounded by a series of thin high-amplitude reflections similar to those observed within Unit 5 on

seismic profile 29. Unit 8 is identified from seismic lines 21 and 28 (Fig. 3.10) and consists of two layers of facies C bounded by thin high-amplitude draping reflections. The base of Unit 8, h8, shows evidence of erosion in form of truncation of underlying strata and small indentations, although the amplitudes of these features are small (~10 m). A layer of facies S pinching out eastward is present in the upper part of Unit 8 and is separated from neighboring units by high-amplitude draping reflections.

3.5.5.2. Interpretation

Character of internal reflections together with erosional bases of Units 6 and 7 suggest that these units were formed as a result of ice advances to the shelf break. The depths of incisions within h6 and h7 are shallow compared with tunnel valleys demonstrated by h1 and h2. However, it still may be possible that these incisions represent distal, shallow parts of a tunnel valley system. The shift in composition of Unit 7 towards layers of mainly transparent facies S implies a period of glacial retreat. Configuration of these layers show a draping pattern, mirroring underlying units and does not show any evidence of grounded ice. Transparency of internal reflections within Unit 7 may indicate poor sediment sorting and/or little change in lithology within the unit. Geometry and facies content of Unit 8 suggest that it may represent evidence of glacial advance. However, very low amplitude of truncation may have been caused by fluvial erosion as well. The transparency of Unit 8 indicates poor sediment sorting and/or constant lithology, which alternatively may represent very coarse, massive sand and gravel deposited as a result of series of outwashes from proglacial systems *[e.g., Back et al., 1998; Kluiving et al., 2003; Erohina et al., 2003]*.

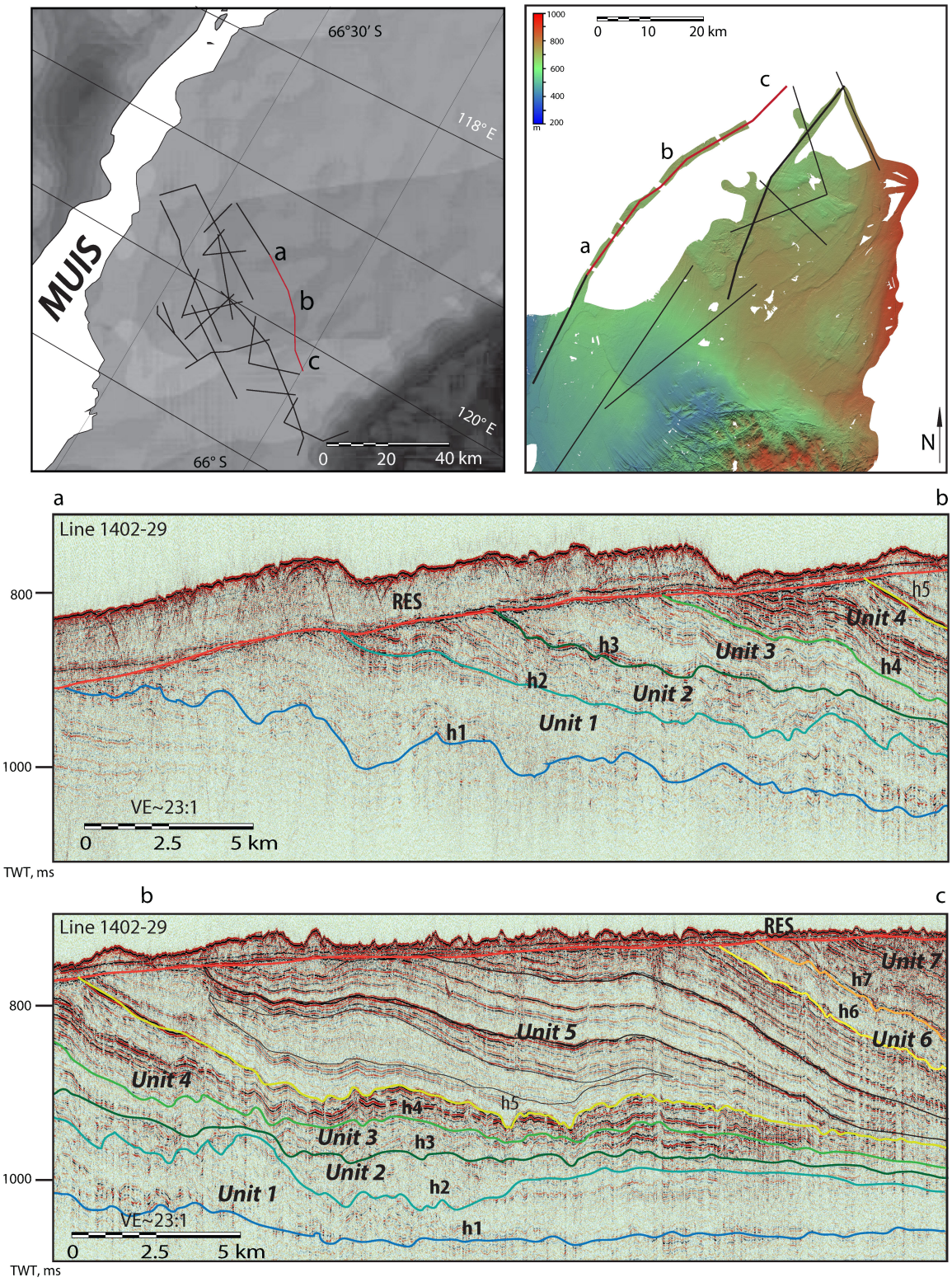

Fig. 3.11. Facies composition and individual erosional surfaces interpreted within MSII from seismic line NBP1402-29.

3.6. Discussion

3.6.1 Sabrina Coast tunnel valley system

Two clear examples of almost symmetric tunnel valley profiles that are found within Unit 2 show similar dimensions. They are ~1150 m wide, ~120 m deep, with flank gradients ranging between 12° and 15° (Fig. 3.12).

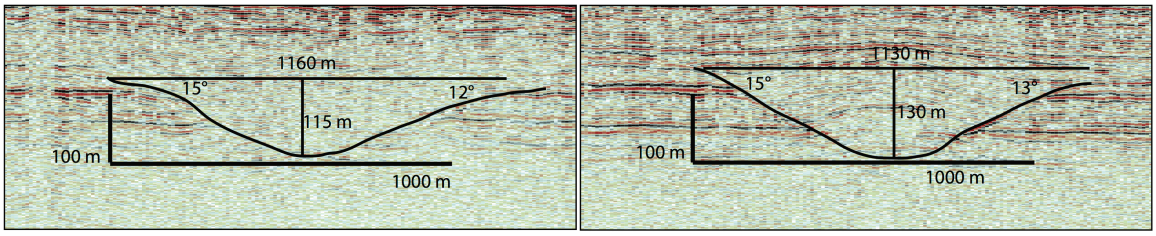

Fig. 3.12. Morphometry of tunnel valleys found within unit 2 of MSII.

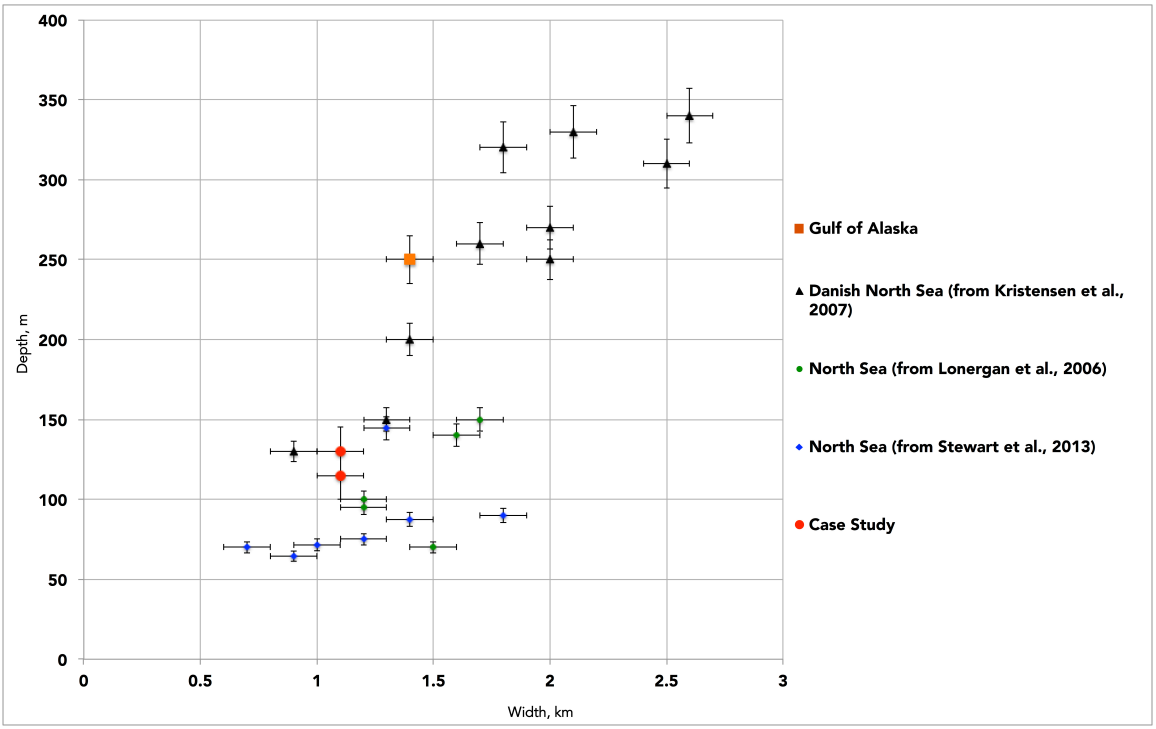

Fig. 3.13. Comparison of morphometry of tunnel valleys from SC shelf and similar features observed in Northern Hemisphere (North Sea and Gulf of Alaska).

Juxtaposition of these parameters with the dimensions of other tunnel valleys found in Northern Hemisphere show that morphometrically, tunnel valleys identified by this study fall within the range of analogs from other polar margins (Fig. 3.13). In addition, asymmetry of channels found updip within the same Unit 2 implies intricate,

anastomosing pattern of these incisions, which is very characteristic of tunnel valleys found across the globe *[e.g., O'Cofaigh, 1996; Huuse and Lykke-Andersen, 2000; Lowe and Anderson, 2002; Denton and Sugden, 2005; Domack et al., 2006; Lonergan et al., 2006; Kristensen et al., 2007; Stewart and Lonergan, 2011]*.

The exact origin of undulating erosional surface (h1) that is interpreted to mark the first expansion of EAIS is difficult to determine confidently due to the limited data coverage. Although there is only one known seismic analog of erosional undulating surface from Antarctic shelves *[Erohina et al., 2004],* studies from Nova Scotia and North Seas provide additional evidence of similar surfaces to represent bases of tunnel valley systems *[e.g., King and Edward, 2001; Lonergan et al., 2006]*. With anastomosing pattern exhibited by tunnel valleys it is more likely that the plane of seismic profile cuts the channel system obliquely and does not capture the cross section of individual valleys, but rather shows the intersection/amalgamation of several channels or simply a part of a longitudinal profile. Such observations, with emphasis on undulating character of longitudinal profiles of tunnel valleys have been widely discussed *[e.g., O'Cofaigh, 1996; Lonergan et al., 2006; Kristensen et al., 2007; Kehew et al., 2012]*.

Comparison of the depth of erosion (~100m) with global sea-level curve *[Miller et al., 2005]* shows that amplitudes of sea-level fluctuations in late Eocene – Oligocene were not larger than ~50 m, which argues against erosion caused by fluvial incision related to the fall in the sea level being the origin of h1. Moreover, numerical isostatic models of Antarctic continent have demonstrated that after the major build-up of ice sheet in late Eocene-early Oligocene inner shelf subsequently subsided and the coasts experienced a progressive relative sea-level rise *[Stocchi et al., 2013]*. Thus, our interpretation of surface h1 is that it more likely represents a part of tunnel valley system formed by first grounded EAIS in the SC shelf. Nevertheless, in order to support this interpretation, more high-resolution seismic data is needed offshore SC shelf, particularly to the west of the study area.

Understanding of the origin of tunnel valleys is important because they provide major drainage pathways for large amounts of subglacial meltwater, which affects basal properties of both hard bedrock and soft sedimentary substrates beneath the ice sheets, playing a significant role in the stability of ice sheets *[e.g., Blankenship et al., 1986;*

Alley et al., 1987; Lowe and Anderson, 2003; Wingham et al., 2006; Siegert et al., 2007]. Therefore, geological and geomorphological information is essential in order to help understand the style, rates and magnitudes of subglacial water flow beneath the AIS *[Smith et al., 2009]*. In their summary of previous Antarctic subglacial meltwater studies, Smith et al. (2009) noted that although several large subglacial drainage systems eroded into bedrock have been found on Antarctic shelves *[e.g., Sugden et al., 1991; Lowe and Anderson, 2003; Denton and Sugden, 2005; Domack et al., 2006]*, there has been no solid evidence of tunnel valleys incised into soft sedimentary substrate. Our results provide first conclusive seismic evidence of at least one preserved, complex, likely extensive tunnel valley system incised into sedimentary deposits at the earliest stage of EAIS evolution.

3.6.2 Sabrina Coast shelf sedimentary architecture and Aurora Basin Complex paleodrainage

Configuration of the SC continental margin shows an overdeepened, tilted inner shelf. Along the dip direction, sedimentary architecture is dominated by progradational foresets and demonstrates gradual increase in slope gradients. Such patterns in architecture of Antarctic shelves have been widely reported from various Antarctic margins and are the consequences of intensive, focused glacial erosion and isostatic loading *[e.g., Eittreim et al., 1995; ten Brink and Schneider, 1995; Bart et al., 2000; Anderson et al., 2001; Bart, 2003; Cooper and O'Brien, 2004; Bart and Iwai, 2012; Livingstone et al., 2012]*. Similar overdeepenings were related to major AIS expansions and excavation of inner shelf by highly erosive ice streams starting from middle Miocene, though the timing of such events differs between the regions (e.g., middle-late Miocene in Prydz Bay *[Cooper and O'Brien, 2004]* and late Pliocene in Antarctic Peninsula *[Bart and Iwai, 2012]*). We suggest that the regional erosional unconformity (RES) that truncates topsets of dipping strata within MSII is related to similar regional event or series of events, which caused subsequent overdeepening. It is not possible to say confidently whether dipping strata found on the current SC shelf represent slope or shelf progradation, because lower resolution, deeper penetrating (basement reaching) seismic data are necessary to locate the initial position of the paleo-shelf break. However, regional seismic data acquired in Antarctic margins that exhibit analogous margin

architecture *[e.g., Cooper et al., 1995; Kristoffersen et al., 2000; Bart et al., 2000; Anderson et al., 2001; Wellner et al., 2001; De Santis et al., 2003; Escutia et al., 2005; Donda et al., 2008]* have shown that that dipping strata represent shelf sequences rather than slope progradation.

Individual units within the MS II show pinch out towards the eastern part of the study area, whereas the dimensions of erosional features found in the western part are larger than those found in the east. These observations suggest that the deposition and erosion at the time of formation of MS II were more intensive to the west from the study area. However, there is no seismic evidence of a sustained ice stream in the study area during deposition of MS II. If there was a paleo-ice stream dominating the erosion and deposition of MS II, we would expect to see a feature that resembles wide, U-shaped trough resulted from erosion by focused ice flow. Instead, the only evidence of such trough is represented by regional erosional surface (RES), which coincides with the eastern flank of modern Reynold's Trough. The absence of paleo-trough may be explained by the following: (a) there was shallower trough that was subsequently deepened/removed by more intensive erosion related to RES; (b) there is evidence of paleo-trough located to the west of the seismic coverage provided by this study; and (c) there was no focused ice stream draining ABC prior to the event related to RES. Since there are no data to support first two hypotheses, we suggest that ABC was drained by series of outlet glaciers, which did not possess ice flux sufficient enough to erode glacial trough and overdeepen the shelf prior the major ice sheet expansion related to RES.

3.6.3 Early ice sheet dynamics in SC

Since the onset of persistent Antarctic Ice Sheet, Sabrina Coast shelf was influenced by glacial system that dominated the drainage of ABC, one of the largest ice basins in the world. Therefore, sedimentary record of Sabrina Coast shelf most likely reflects fluctuations of both local and regional ice since the initiation of ice sheet and holds clues on the regional climatic history. Our seismic analysis from the Sabrina Coast continental shelf suggests a dynamic glacial evolution including expansions of the EAIS across the inner and mid-shelf on at least eight occasions (erosional surfaces h1-h8) in the late Paleogene-early Neogene. Differences in facies composition and architecture of sequences composing MSII suggest glacial fluctuations of considerable magnitudes.

First grounded EAIS is expressed through the deep (~100 m) erosional undulating surface (h1) that may represent a part of subglacial meltwater channel system. After the initial polythermal expansion, ice sheet significantly retreated and the shelf experienced long period of warmer, open-marine conditions marked by thick layer of stratified sediment (Unit 1). At least three deep, stacked erosional surfaces (h2,h2.2,h3) suggest major expansion of EAIS that consisted of series of ice front oscillations across the shelf. First clear evidence of subglacial tunnel valley system within the Unit 2 proves the aggressive, polythermal style of these glaciations. Seismic character of sequences above (Units 3-5) document series of predominantly ice-free conditions interrupted by short pulses of few minor expansions of shelf-grounded ice sheet. Units 6-7 suggest another ice sheet expansion, with at least two events of glacial erosion (slightly more aggressive than observed within Units 3-5) followed by period of ice retreat. Last documented erosion is provided by h8 and may reflect glacial advance close to the inner shelf, but shelf-grounded event is less likely since no conclusive evidence of grounded ice has been found. Further history is obscured due to: (1) data lacking in the outer shelf and (2) prominent erosional event that marks major glacial expansion and transition to a polar ice sheet.

3.6.4. Ice sheet dynamics in SC and linkages to global climate

The analysis of geomorphological features in the SC indicates a long and variable history of glacial erosion and sedimentation, which in turn raises major questions about what caused this variability to occur. Previous high-resolution studies from Antarctic continental shelves have indicated that grounded ice has covered much of Antarctica since early Oligocene times with fluctuations of ice sheets largely reflecting oscillations in orbital cycles *[e.g., Hambrey et al., 1991; Zachos et al., 1997; Zachos et al., 2001; Naish et al., 2001]*. Juxtaposition with global climate records can help resolve the nature of long-term changes in amplitudes and frequencies of ice sheet erosion and sedimentation observed in SC shelf. Although the resolution of age constraints provided by this study is very limited and therefore inadequate to link individual stratigraphic and climate events, it is sufficient to put the fluctuations of EAIS observed in SC into general global climate context (Fig. 3.14).

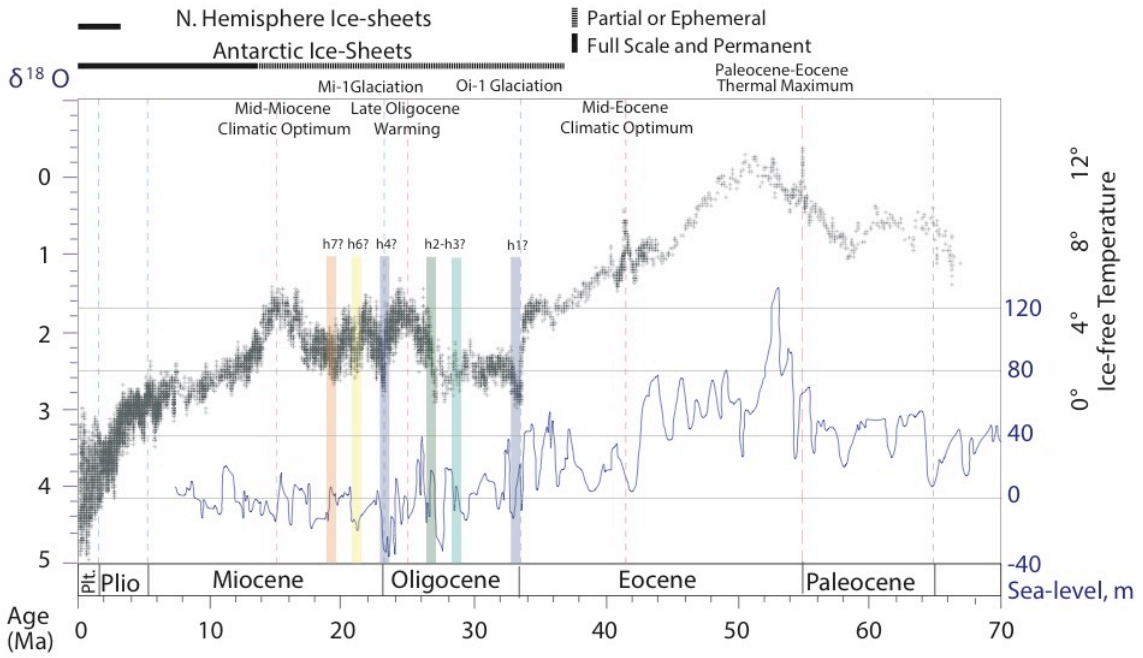

Fig. 3.14. Proposed possible timing of erosional events related to major glacial expansions in Sabrina Coast in Oligocene-middle Miocene juxtaposed with global oxygen isotope curve by Zachos et al., (2001) and global sea-level curve by Miller et al., (2005).

We use the global oxygen isotope curve as a proxy for global ice volume *[Zachos et al., 2001]* together with global sea-level curve *[Miller et al., 2005]* to discuss possible timing of events interpreted from high-resolution seismic data. Late Eocene ice rafted debris (IRD) recovered from core 55 just below h1 suggest that the erosional event related to undulating surface h1 occurred not long after the late Eocene. Assuming this first shelf-grounded ice expansion was in phase with global orbital trends, such event may have occurred as a result of Oi-1 glacial event (Fig. 3.14). Thickness of ice-distal Unit 1 deposited on top of h1 requires sufficient time of interglacial conditions, which may be represented by early Oligocene warming. Three consecutive erosional surfaces h2, h2.2 and h3 fit with the pattern of the global oxygen isotope curve predating late Oligocene warming. Similarly to Unit 1, ice-distal Unit 3 required long period of warm conditions, which may have been provided by the late Oligocene warming. The core 59 acquired along profile 21 suggests that sediments just above h6 are of Miocene age. We speculate that the following glacial events related to h4, h5, h6 and h7 occurred during the several glacial expansions between Mi-1 glacial event and Mid-Miocene Climatic Optimum.

In general, proposed glacial dynamics fits δO^{18} curve for Oligocene-early Miocene (Fig. 3.14). Magnitudes of ice sheet oscillations might provide a possible explanation for observed differences in intensity of erosion observed within SC shelf. Thus, the deepest erosion events related to surfaces h1 and h2 could be explained by colder climates dominating early Oligocene as compared to the late Oligocene - early Miocene.

Additional explanation for high amplitudes of early glacial erosion arises from paleoenvironmental considerations. By the early Eocene, the opening of Tasmanian Gateway has already started, allowing the development of shallow marginal seas *[Stickley et al., 2004]*. Paleooceanographic studies have shown that the Eocene Pacific Southern Ocean was dominated by clockwise gyres *[Sloan and Huber, 2001; Huber et al., 2004]*. Considering that the Wilkes Land together with its highlands was of higher elevation compared to the current bed topography *[e.g., Stochhi et al., 2013]*, such paleogeographic setting may have favored the development of temperate climates with likely some winter snow *[Francis, 1999; 2000]*. As climate cooled down rapidly as a result of Oi-1 event, it might have allowed more snow to accumulate and develop glacial systems similar to those currently observed in the Gulf of Alaska, with very dynamic, aggressive, likely tidewater glaciers. Such a setting could provide additional explanation for the occurrence of deep, meltwater related, first glacial erosion observed in SC as well as similarity of some features found within early glacial strata to those of Gulf of Alaska.

3.7. Conclusions

First high-resolution seismic data acquired on the Sabrina Coast shelf have revealed major transitions in glacial regime of the EAIS. Three large-scale megasequences represent changes in the dominant pattern of sedimentation: Megasequence I shows signs of fluvial and possibly glacio-fluvial sedimentation; Megasequence II provides evidence of polythermal glacial sedimentation with significant amount of meltwater; Megasequence III overlies the regional erosional surface that marks major ice sheet expansion and transition into polar ice sheet glacial regime with no significant evidence of subglacial meltwater preserved.

Megasequence II exhibits preserved record of EAIS evolution starting from its first expansion. Seismic stratigraphic analysis suggests a dynamic glacial late Paleogene-

early Neogene evolution including expansions of the EAIS across the shelf at least eight times, which is marked by erosional surfaces and chaotic acoustic character of overlying strata. We report on finding first conclusive evidence of deep, extensive tunnel valley system incised into sedimentary substrate around continental margins of Antarctic continent. The Sabrina Coast tunnel valley system was formed presumably during Oligocene as a result of second major EAIS shelf expansion. Shallower erosion events observed in the upper part of Megasequence II suggest more extensive glaciations in the Oligocene compared to the Miocene.

We suggest that eight glacial expansions have occurred between Oi-1 glaciation event and Mid-Miocene Climatic Optimum. However, age constraints of better quality are essential to make conclusive interpretations on timing of glacial history of EAIS in Sabrina Coast. Dipping strata comprising the shelf together with well-preserved, striking morphological features make this area a perfect target for the future investigations, particularly scientific drilling programs, which could provide further, detailed evidence of dynamic EAIS behavior and elucidate major transitions in the history of global and regional climate.

References

Aitken, A., D. Young, F. Ferraccioli, P. Betts, J. Greenbaum, T. Richter, J. Roberts, D. Blankenship, and M. Siegert (2014), The subglacial geology of Wilkes Land, East Antarctica, *Geophys. Res. Lett.*, *41*(7), 2390–2400, doi:10.1002/2014GL059405.

Alley, R. B., D. D. Blankenship, C. R. Bentley and S.T. Rooney. 1987a. Till beneath Ice Stream B. 3. Till deformation: evidence and implications. *J. Geophys. Res.*, **92**(B9), 8921-8929.

Alley, R. B., Clark, P. U., Huybrechts, P., & Joughin, I. (2005). Ice-sheet and sea-level changes. *Science*, *310*(5747), 456-460.

Alley, R. B., Anandakrishnan, S., Dupont, T. K., Parizek, B. R. & Pollard, D. Effect of sedimentation on ice-sheet grounding-line stability. *Science* 315, 1838–41 (2007).

Anderson, J. B., & Bartek, L. R. (1992). Cenozoic glacial history of the Ross Sea revealed by intermediate resolution seismic reflection data combined with drill site information. *The Antarctic Paleoenvironment: A Perspective on Global Change: Part One*, 231-264.

Anderson, J.B., 1999, Antarctic marine geology: Cambridge, Cambridge University Press.

Anderson, J. B., Shipp, S. S., Lowe, A. L., Wellner, J. S., & Mosola, A. B. (2002). The Antarctic Ice Sheet during the Last Glacial Maximum and its subsequent retreat history: a review. *Quaternary Science Reviews*, *21*(1), 49-70.

Back, S., De Batist, M., Strecker, M. R., & Vanhauwaert, P. (1999). Quaternary depositional systems in northern Lake Baikal, Siberia. *The Journal of Geology*, *107*(1), 1-12.

Bamber, J. L., Vaughan, D. G., & Joughin, I. (2000). Widespread complex flow in the interior of the Antarctic ice sheet. *Science*, *287*(5456), 1248-1250.

Bart, P. J., Anderson, J. B., Trincardi, F., & Shipp, S. S. (2000). Seismic data from the Northern basin, Ross Sea, record extreme expansions of the East Antarctic Ice Sheet during the late Neogene. *Marine Geology*, *166*(1), 31-50.

Bart, P. J., & Iwai, M. (2012). The overdeepening hypothesis: How erosional modification of the marine-scape during the early Pliocene altered glacial dynamics on the Antarctic Peninsula's Pacific margin. *Palaeogeography, Palaeoclimatology, Palaeoecology*, *335*, 42-51.

Batchelor, C. L., Dowdeswell, J. A., & Pietras, J. T. (2013). Variable history of Quaternary ice-sheet advance across the Beaufort Sea margin, Arctic Ocean.*Geology*, *41*(2), 131-134.

Batchelor, C. L., Dowdeswell, J. A., & Pietras, J. T. (2014). Evidence for multiple Quaternary ice advances and fan development from the Amundsen Gulf cross-shelf trough and slope, Canadian Beaufort Sea margin. *Marine and Petroleum Geology*, *52*, 125-143.

Berger, A., Gulick, S., Spotila, J., Upton, P., Jaeger, J., Chapman, J., Worthington, L., Pavlis, T., Ridgway, K., Willems, B., and McAleer, R., 2008, Quaternary tectonic response to intensified glacial erosion in an orogenic wedge: Nature Geoscience, v. 1, no. 11, p. 793799, doi: 10.1038/ngeo334.

Blankenship, D., Bentley, C., Rooney, S. & Alley, R. Seismic measurements reveal a saturated porous layer beneath an active Antarctic ice stream. *Nature* 322, 54–57 (1986).

Boulton, G.S., 1986, Push-moraines and glacier-contact fans in marine and terrestrial environments: Sedimentol- ogy, v. 33, p. 677–698, doi: 10.1111/j.1365-3091.1986. tb01969.x.

Briner, J., Bini, A., and Anderson, R., 2009, Rapid early Holocene retreat of a Laurentide outlet glacier through an Arctic fjord: Nature Geoscience, v. 2, no. 7, p. 496–499, doi: 10.1038/ngeo556.

Briner, J.P., and Kaufman, D.S., 2008, Late Pleistocene mountain glaciation in Alaska: key chronologies: Journal of Quaternary Science, doi: 10.1002/jqs.1196.

Butt, F. A., Elverhøi, A., Forsberg, C. F. & Solheim A.: Evolution of the Scoresby Sund Fan, central East Greenland- evidence from ODP Site 987. *Norsk Geologisk Tidsskrift*, Vol81, pp. 3-15. (2001).

Cai, J., Powell, R. D., Cowan, E. A., & Carlson, P. R. (1997). Lithofacies and seismic-reflection interpretation of temperate glacimarine sedimentation in Tarr Inlet, Glacier Bay, Alaska. *Marine Geology*, *143*(1), 5-37.

Carlson, P.R., 1989, Seismic reflection characteristics of glacial and glacimarine sediment in the Gulf of Alaska and adjacent fjords: Marine Geology, v 85, p. 391– 416, doi: 10.1016/0025-3227(89)90161-8.

Church, J. A., & White, N. J. (2011). Sea-level rise from the late 19th to the early 21st century. *Surveys in Geophysics*, *32*(4-5), 585-602.

Clark, C.D., 1993, Mega-scale glacial lineations and cross-cutting ice-flow landforms: Earth Surface Processes and Landforms, v. 18, p. 1–19, doi: 10.1002/ esp.3290180102.

Clark, C., Evans, D. & Piotrowski, J. Palaeo-ice streams: an introduction. Boreas 32, 1–3 (2003).

Close, D. (2010), Slope and fan deposition in deep-water turbidite systems, East Antarctica, *Marine Geology*, *274*(1-4), 2131, doi:10.1016/j.margeo.2010.03.002.

Close, D., H. Stagg, and P. O'Brien (2007), Seismic stratigraphy and sediment distribution on the Wilkes Land and Terre Adélie margins, East Antarctica, *Marine Geology*, *239*(1-2), 3357, doi:10.1016/j.margeo.2006.12.010.

Colwell, J.B., Stagg, H.M.J., Direen, N.G., Bernardel, G., Borissova, I., 2006. The structure of the continental margin off Wilkes Land and Terre Adélie, East Antarctica. In: Fütterer, D.K., Damaske, D., Kleinschmidt, G., Miller, H., Tessensohn, F. (Eds.), Antarctica: Contributions to Global Earth Sciences. Springer-Verlag, Berlin, pp. 327–340.

Cooper, A. K., Barker, P. F., & Brancolini, G. (Eds). (1995). Geology and Seismic Stratigraphy of the Antarctic Margin. American Geophysical Union, Washington, DC, Antarctic Research Series, Vol. 68.

Cooper, A.K., O'Brien, P.E., 2004. Leg 188 synthesis: transitions in the glacial history of the Prydz Bay region, East Antarctica, from ODP drilling. In: Cooper, A.K., O'Brien, P.E., Richter, C. (Eds.), Proceedings of the ODP, Scientific Results, 188, pp. 1–42. College Station, Texas.

Conway, H., Hall, B.L., Denton, G.H., Gades, A.M., and Waddington, E.D., 1999. Past and future grounding-line retreat of the West Antarctic Ice Sheet, Science, 286, 280-283.

De Angelis, H, and P. Skvarca, 2003: Glacier surge after ice shelf collapse. *Science,* 299, 1560-1562.

De Santis, L., Brancolini, G., Donda, F., 2003. Seismo-stratigraphic analysis of the Wilkes Land continental margin (East Antarctica): influence of glacially driven processes on the Cenozoic deposition. Deep-Sea Research II 50 (8–9), 1563–1594.

Denton, G.H., Sugden, D.E., 2005. Meltwater features that suggest Miocene ice-sheet overriding of the Transantarctic Mountains in Victoria Land, Antarctica. Geogr. Ann. 87A, 67–85.

Domack, E., Amblas, D., Gilbert, R., Brachfeld, S., Camerlenghi, A., Rebessco, M., Canals, M., 2006. Subglacial morphology and glacial evolution of the Palmer Deep outlet system, Antarctic Peninsula. Geomorphology 75, 125–142.

Donda, F., P. O'Brien, L. Santis, M. Rebesco, and G. Brancolini (2008), Mass wasting processes in the Western Wilkes Land margin: Possible implications for East Antarctic

glacial history, *Palaeogeography, Palaeoclimatology, Palaeoecology*, *260*(1-2), 7791, doi:10.1016/j.palaeo.2007.08.008.

Dowdeswell, J.A., and Ó Cofaigh, C., 2002., Glacier- influenced sedimentation on high-latitude continental margins: The Geological Society of London, Special Publication, v. 203, p. 277–304.

Dowdeswell, J.A., and Elverhøi, A., 2002, The timing of initiation of fast-flowing ice streams during a glacial cycle inferred from glacimarine sedimenta- tion: Marine Geology, v. 188, p. 3–14, doi: 10.1016/ S0025-3227(02)00272-4.

Dowdeswell, J.A., Ó Cofaigh, C., and Pudsey, C.J., 2004, Thickness and extent of the subglacial till layer beneath an Antarctic paleo-ice stream: Geology, v. 32, p. 13–16.

Dowdeswell, J. Atmospheric Science: The Greenland Ice Sheet and Global Sea-Level Rise.Science 311, 963–964 (2006).

Dowdeswell, J.A., Ottesen, D., Rise, L., Craig, J., 2007. Identification and preservation of landforms diagnostic of past ice-sheet activity on continental shelves from three-dimensional seismic evidence. Geology 35, 359-362.

Dowdeswell, J., Ottesen, D., and Rise, L., 2010, Rates of sediment delivery from the Fennoscandian Ice Sheet through an ice age: Geology, v. 38, no. 1, p. 36, doi: 10.1130/G25523.1.

Dowdeswell, J. & Fugelli, E. The seismic architecture and geometry of grounding-zone wedges formed at the marine margins of past ice sheets. *Geological Society of America Bulletin* 124, 17501761 (2012).

Dowdeswell, J. A., Hogan, K. A., Cofaigh, C. Ó., Fugelli, E. M. G., Evans, J., & Noormets, R. (2014). Late Quaternary ice flow in a West Greenland fjord and cross-shelf trough system: submarine landforms from Rink Isbrae to Uummannaq shelf and slope. *Quaternary Science Reviews*, *92*, 292-309.

Drewry, D. J., & Meldrum, D. T. (1978). Antarctic airborne radio echo sounding, 1977–78. *Polar Record*, *19*(120), 267-273.

Erohina, T., Cooper, A., Handwerger,D., and Dunbar, R., 2004. Seismic stratigraphic correlations between ODP Sites 742 and 1166: implications for depositional paleoenvironments in Prydz Bay, Antarctica. In Cooper, A.K., O'Brien, P.E., and Richter, C. (Eds.), Proc. ODP, Sci. Results, 188, 1–21

Eittreim, S.L., Smith, G.L., 1987. Seismic Sequences and Their Distribution on the Wilkes Land Margin. In: Eittreim, S.L., Hampton, M.A. (Eds.), The Antarctic Continental Margin Geology and Geophysics of Offshore Wilkes Land. Circum-Pacific Council for Energy and Mineral, Houston, Texas, USA, pp. 14–43.

Elmore, C., Gulick, S., Willems, B., and Powell, R., 2013, Seismic stratigraphic evidence for glacial expanse during glacial maxima in the Yakutat Bay Region, Gulf of Alaska: Geochemistry, Geophysics, Geosystems, doi: 10.1002/ggge.20097.

Elverhøi, A., Dowdeswell, J., Funder, S., Mangerud, J. & Stein, R. Glacial And Oceanic History Of The Polar North Atlantic Margins: An Overview. *Quaternary Science Reviews* 17, 110 (1998).

Elverhøi, A., Hooke, R.L., and Solheim, A. Late Cenozoic erosion and sediment yield from the Svalbard-Barents Sea region: Implications for understanding erosion of glacierized basins: *Quaternary Science Reviews,* v. 17, p. 209–241, (1998).

Escutia, C., De Santis, L., Donda, F., Dunbar, R.B., Cooper, A.K., Brancolini, G., Eittreim, S.L., 2005. Cenozoic ice sheet history from East Antarctic Wilkes Land continental margin sediments. Global and Planetary Change 45, 51–81.

Florindo, F., & Siegert, M. (Eds.). (2008). *Antarctic climate evolution* (Vol. 8). Elsevier.

Flower, B. P., & Kennett, J. P. (1994). The middle Miocene climatic transition: East Antarctic Ice Sheet development, deep ocean circulation and global carbon cycling. Palaeogeogr. Palaeoclimatol. Palaeoecol., 108, 537–555.

Francis, J. E. (1999). Evidence from fossil plants for Antarctic palaeoclimates over the past 100 million years. In: P. J. Barrett, & G. Orombelli (Eds). Geological Records of Global and Planetary Changes. Terra Antartica Report 3, Siena, Italy, pp. 43–52.

Francis, J. E. (2000). Fossil wood from Eocene high latitude forests, McMurdo Sound, Antarctica. In: J. D. Stilwell, & R. M. Feldmann (Eds). Paleobiology and Palaeoenvironments of Eocene Rocks, McMurdo Sound, East Antarctica. Antarctic Research Series. American Geophysical Union, Washington, DC, Vol. 76, pp. 253–260.

Francis J.E., Marenssi S., Levy R., Hambrey M., Thorn V.C., Mohr B., Brinkhuis H., Warnaar J., Zachos J., Bohaty S., DeConto R., (2008) Chapter 8 From Greenhouse to Icehouse - The Eocene/Oligocene in Antarctica,*Developments in Earth and Environmental Sciences*, 8, pp.309-368.

Fretwell, P., et al. (2013), Bedmap2: Improved ice bed, surface and thickness datasets for Antarctica, Cryosphere, 7(1), 375–393.

Gulick, S., Lowe, L., Pavlis, T., Gardner, J., and Mayer, L., 2007, Geophysical insights into the Transition fault debate: Propagating strike slip in response to stalling Yakutat block subduction in the Gulf of Alaska: Geology, v. 35, no. 8, p. 763, doi: 10.1130/G23585A.1.

Gulick, S.P.S., Reece, R.S., Christeson, G.L., van Avendonk, H., Worthington, L.L., Pavlis, T.L., Transition Fault and the unstable Yakutat-Pacific-North American triple junction: Geology, v 41, p. 571-574, DOI:10.1130/G33900.1, 2013.

Hambrey, M.J., Ehrmann, W.U., and Larsen, B., 1991. Cenozoic glacial record of the Prydz Bay continental shelf, East Antarctica. In Barron, J., Larsen, B., et al., Proc. ODP, Sci. Results, 119: College Station, TX (Ocean Drilling Program), 77–132.

Huber, M., & Sloan, L. C. (2001). Heat transport, deep waters, and thermal gradients: Coupled simulation of an Eocene greenhouse climate. Geophys. Res. Lett., 28, 3481–3484.

Huber, M., Brinkhuis, H., Stickley, C. E., Do¨o¨s, K., Sluijs, A., Warnaar, J., Schellenberg, S. A., & Williams, G. L. (2004). Eocene circulation of the Southern Ocean: Was Antarctica kept warm by subtropical waters? Paleoceanography, 19(4), PA4026, doi:10.1029/2004PA001014.

Huuse, M., Lykke-Andersen, H., 2000. Overdeepened Quaternary valleys in the eastern Danish North Sea: morphology and origin. Quat. Sci. Rev. 19, 1233–1253.

Intergovernmental Panel on Climate Change, ed. *Climate Change 2013: The Physical Science Basis: Working Group I Contribution to the Fifth Assessment Report of the Intergovernmental Panel on Climate Change*. Cambridge University Press, 2014.

Jamieson, S., Sugden, D. & Hulton, N. The evolution of the subglacial landscape of Antarctica.*Earth and Planetary Science Letters* 293, 127 (2010).

Jamieson, S. *et al.* Ice-stream stability on a reverse bed slope. *Nature Geosci* 5, 799–802 (2012).

Jaeger, J.M., Gulick, S.P.S., LeVay, L.J., and the Expedition 341 Scientists, 2014, *Proc. IODP*, 341: College Station, TX (Integrated Ocean Drilling Program). doi:10.2204/iodp.proc.341.2014

Kehew, A. E., Piotrowski, J. A., & Jørgensen, F. (2012). Tunnel valleys: Concepts and controversies—A review. *Earth-Science Reviews*, *113*(1), 33-58.

King, Edward L., (2001), A glacial origin for Sable Island: ice and sea-level fluctuations from seismic stratigraphy on Sable Island Bank, Scotian Shelf, offshore Nova Scotia. Natural Resources Canada, Geological Survey of Canada.

Kluiving, S., J. Bosch, J. Ebbing, C. Mesdag, and R. Westerhoff (2003), Onshore and offshore seismic and lithostratigraphic analysis of a deeply incised Quaternary buried valley system in the Northern Netherlands, *Journal of Applied Geophysics*, *53*(4), 249271, doi:10.1016/j.jappgeo.2003.08.002.

Laberg, J., Andreassen, K., Knies, J., Vorren, T., and Winsborrow, M., 2010, Late Pliocene-Pleistocene development of the Barents Sea Ice Sheet: Geology, v. 38, no. 2, p. 107110, doi: 10.1130/G30193.1.

Lagoe, M.B., Eyles, C.H., and Eyles, N., 1993, Timing of late Cenozoic tidewater glaciation in the far North Pacific: Geological Society of America Bulletin, doi: 10.1130/0016-7606(1993)105<1542:TOLCTG>2.3.CO;2.

Larter, R.D., Anderson, J.B., Graham, A.G.C., Gohl, K., Hillenbrand, C.-D., Jakobsson, M., Johnson, J.S., Kuhn, G., Nitsche, F.O., Smith, J.A., Witus, A.E., Bentley, M.J., Dowdeswell, J.A., Ehrmann, W., Klages, J.P., Lindow, J., O Cofaigh, C., Spiegel, C., 2014. Reconstruction of changes in the Amundsen Sea and Bellingshausen Sea sector of the West Antarctic Ice Sheet since the Last Glacial Maximum. Quat. Sci. Rev. 100, 55, 86.

Lawver, L., & Gahagan, L. M. (2003). Evolution of Cenozoic seaways in the circum-Antarctic region. Palaeogeogr. Palaeoclimatol. Palaeoecol., 198, 11–37.

Lisiecki, L., and Raymo, M., 2005, A Pliocene-Pleistocene stack of 57 globally distributed benthic δ18O records: Paleoceanography, v. 20, no. 1, doi: 10.1029/2004PA001071.

Livingstone, S. J., Cofaigh, C. Ó., Stokes, C. R., Hillenbrand, C. D., Vieli, A., & Jamieson, S. S. (2012). Antarctic palaeo-ice streams. *Earth-Science Reviews*,*111*(1), 90-128.

Lonergan, L., Maidment, S.C.R., Collier, J.S., 2006. Pleistocene subglacial tunnel valleys in the central North Sea basin: 3-D morphology and evolution. J. Quat. Sci. 21, 891–903.

Lowe, A. L., & Anderson, J. B. (2003). Evidence for abundant subglacial meltwater beneath the paleo-ice sheet in Pine Island Bay, Antarctica. *Journal of Glaciology*, *49*(164), 125-138.

McClymont, E. L., Sodian, S. M., Rosell-Melé, A., Rosenthal, Y., 2013, Pleistocene sea-surface temperature evolution: Early cooling, delayed glacial intensification, and implications for the mid-Pleistocene climate transition. Earth Science Reviews, v. 123, p. 173-193.

Meigs, A., and Sauber, J., 2000, Southern Alaska as an example of the long-term consequences of mountain building under the influence of glaciers: Quaternary Science Reviews, v. 19, no. 14-15, p. 15431562, doi: 10.1016/S0277-3791(00)00077-9.

Miller, K. G., Kominz, M. A., Browning, J. V., Wright, J. D., Mountain, G. S., Katz, M. E., & Pekar, S. F. (2005). The Phanerozoic record of global sea-level change. *science*, *310*(5752), 1293-1298.

Molnia, B., and Post, A., 2010, Introduction to the Bering Glacier System, Alaska/Canada: Early observations and scientific investigations, and key geographic features: Geological Society of America Special Papers, v. 462, p. 13–42, doi: 10.1130/2010.246202.

Naish, T. R., Woolfe, K. J., Barrett, P. J., Wilson, G. S., Atkins, C., Bohaty, S. M., ... & Wonik, T. (2001). Orbitally induced oscillations in the East Antarctic ice sheet at the Oligocene/Miocene boundary. *Nature*, *413*(6857), 719-723.

Nielsen, T. *et al.* A comparison of the NW European glaciated margin with other glaciated margins. *Marine and Petroleum Geology* 22, 11491183 (2005).

O'Brien, P. E., De Santis, L., Harris, P. T., Domack, E. & Quilty, P. G. 1999: Ice shelf grounding zone features of western Prydz Bay, Antarctica: sedimentary processes from seismic and sidescan images. *Antarctic Science 11*, 78–91.

O'Brien, P.E., Stanley, S., Parums, R., 2006. Post-rift continental slope and rise sediments from 38°E to 164°E, East Antarctica. In: Fütterer, D.K., Damaske, D., Kleinschmidt, G., Miller, H., Tessensohn, F. (Eds.), Antarctica: Contributions to Global Earth Sciences. Springer-Verlag, Berlin, pp. 341–347.

Ó Cofaigh, C., 1996. Tunnel valley genesis. Prog. Phys. Geogr. 20, 1–19.

Ó Cofaigh, C., Pudsey, C.J., Dowdeswell, J.A. and Morris, P., 2002, Evolution of subglacial bedforms along a paleo-ice stream, Antarctic Peninsula continental shelf: Geophysical Research Letters, v. 29, doi: 10.1029/2001GL014488.

Ó Cofaigh, C., Taylor, J., Dowdeswell, J.A., Pudsey, C.J., 2003. Palaeo-ice streams, trough mouth fans and high-latitude continental slope sedimentation. Boreas 32, 37e55.

Ó Cofaigh, C., Dowdeswell, J.A., Allen, C.S., Hiemstra, J., Pudsey, C.J., Evans, J., and Evans, D.J.A., 2005, Flow dynamics and till genesis associated with a marine-based Antarctic palaeo-ice stream: Quaternary Science Reviews, v. 24, p. 709–740.

O'Cofaigh, C. *et al.* Glacimarine lithofacies, provenance and depositional processes on a West Greenland trough-mouth fan. *J. Quaternary Sci.* 28, 13–26 (2013).

O Grady, D. B., & Syvitski, J. P. (2002). Large-scale morphology of Arctic continental slopes: the influence of sediment delivery on slope form. *Special Publication-Geological Society Of London*, *203*, 11-32.

Ottesen, D., Dowdeswell, J.A., and Rise, L., 2005, Submarine landforms and the reconstruction of fast-flowing ice streams within a large Quater- nary ice sheet: The 2500-km-long Norwegian- Svalbard margin (57o to 80oN): Geological Society of America Bulletin

Ottesen, D., and Dowdeswell, J., 2006, Assemblages of submarine landforms produced by tidewater glaciers in Svalbard: Journal of Geophysical Research, v. 111, no. F1, doi: 10.1029/2005JF000330.

Ottesen, D., Dowdeswell, J.A., Lanvik, J.Y., Mienert, J., 2007. Dynamics of the Late Weichselian ice sheet on Svalbard inferred from high-resolution sea-floor morphology. Boreas 36, 286e306.

Ottesen, D., Dowdeswell, J.A., 2009. An inter-ice stream glaciated margin: subma- rine landforms and a geomorphic model based on marine-geophysical data from Svalbard. Geol. Soc. Am. Bull. 121, 1647e1665.

Plafker, G., Moore, J.C., and Winkler, G.R., 1994, Geology of the southern Alaska margin, in Plafker, G., and Berg, H.C., eds., The geology of Alaska: Boulder, Colorado, Geological Society of America, Geology of North America, v. G-1, p. 389–449.

Pritchard, H., R. Arthern, D. Vaughan, and L. Edwards (2009), Extensive dynamic thinning on the margins of the Greenland and Antarctic ice sheets., *Nature*, *461*(7266), 971–5, doi:10.1038/nature08471.

Powell, R. D., & Cooper, J. M. (2002). A glacial sequence stratigraphic model for temperate, glaciated continental shelves. *Geological Society, London, Special Publications*, *203*(1), 215-244.

Rebesco, M., A. Camerlenghi, R. Geletti, and M. Canals (2006), Margin architecture reveals the transition to the modern Antarctic ice sheet ca. 3 Ma, *Geology*, *34*(4), 301, doi:10.1130/G22000.1.

Rignot, E. (1998), Fast recession of a West Antarcitc glacier, Science, 281, 549 – 551.

Rignot, E., J. Bamber, M. Broeke, C. Davis, Y. Li, W. Berg, and E. Meijgaard (2008), Recent Antarctic ice mass loss from radar interferometry and regional climate modelling,*Nature Geoscience*, *1*(2), 106–110, doi:10.1038/ngeo102.

Rignot, E., Mouginot, J., & Scheuchl, B. (2011). Ice flow of the Antarctic ice sheet. *Science*, *333*(6048), 1427-1430.

Rignot, E., Jacobs, S., Mouginot, J., & Scheuchl, B. (2013). Ice-shelf melting around Antarctica. *Science*, *341*(6143), 266-270.

Sheaf, M., Serpa, L., and Pavlis, T., 2003, Exhumation rates in the St. Elias Mountains, Alaska: Tectonophysics, v. 367, no. 1-2, p. 111, doi: 10.1016/S0040-1951(03)00124-0.

Shepherd, A. & Wingham, D. Recent sea-level contributions of the Antarctic and Greenland ice sheets. *Science* 315, 1529–32 (2007).

Shipp, S., J. Anderson, and E. Domack (1999), Late Pleistocene–Holocene retreat of the West Antarctic .pdf, *Geological Society of America Bulletin*, *111*(10), 1486, doi:10.1130/0016-7606(1999)111<1486:LPHROT>2.3.CO;2.

Shipp, S.S., Wellner, J.S., and Anderson, J.B., 2002, Retreat signature of a polar ice stream: Sub-glacial geomorphic features and sediments from the Ross Sea, Antarctica

Siegert, M., Dowdeswell, J., and Melles, M., 1999, Late Weichselian Glaciation of the Russian High Arctic: Quaternary Research, v. 52, no. 3, p. 273-285, doi: 10.1006/qres.1999.2082.

Siegert, M., J. Taylor, and A. Payne (2005), Spectral roughness of subglacial topography and implications for former ice-sheet dynamics in East Antarctica, *Global and Planetary Change*, *45*(1-3), 249263, doi:10.1016/j.gloplacha.2004.09.008.

Siegert, M.J., Le Brocq, A., Payne, A., 2007. Hydrological connections between Antarctic subglacial lakes and the flow of water beneath the East Antarctic Ice Sheet. In: Hambrey, M.J., Christoffersen, P., Glasser, N.F., Hubbard, B.P. (Eds.), Glacial Sedimentary Processes and Special Publication #39. International Association of Sedimentologists, pp. 3–10.

Smith, J. A., Hillenbrand, C. D., Larter, R. D., Graham, A. G., & Kuhn, G. (2009). The sediment infill of subglacial meltwater channels on the West Antarctic continental shelf. *Quaternary Research*, *71*(2), 190-200.

Steffensen, J. P., Andersen, K. K., Bigler, M., Clausen, H. B., Dahl-Jensen, D., Fischer, H., & White, J. W. (2008). High-resolution Greenland ice core data show abrupt climate change happens in few years. *Science*, *321*(5889), 680-684.

Stewart, M., Lonergan, L., & Hampson, G. (2012). 3D seismic analysis of buried tunnel valleys in the Central North Sea: tunnel valley fill sedimentary architecture. *Geological Society, London, Special Publications*, *368*(1), 173-184.

Stickley, C. E., H. Brinkhuis, S. A. Schellenberg, A. Sluijs, U. Ro¨hl, M. Fuller, M. Grauert, M. Huber, J. Warnaar, and G. L. Williams (2004), Timing and nature of the deepening of the Tasmanian Gateway, Paleoceanography, 19, PA4027, doi:10.1029/2004PA001022

Stocchi, P., Escutia, C., Houben, A. J., Vermeersen, B. L., Bijl, P. K., Brinkhuis, H., ... & Yamane, M. (2013). Relative sea-level rise around East Antarctica during Oligocene glaciation. *Nature Geoscience*, *6*(5), 380-384.

Stokes, C.R., Clark, C.D., 2001. Palaeo-ice streams. Quat. Sci. Rev. 20, 1437-1457.

Stokes, C.R., Clark, C., Winsborrow, M., 2006. Subglacial bedform evidence for a

major palaeo-ice stream in Amundsen Gulf and its retreat phases, Canadian Arctic Archipelago. J. Quat. Sci. 21, 399-412.

Stokes, C., Corner, G., Winsborrow, M., Husum, K., and Andreassen, K., 2014, Asynchronous response of marine-terminating outlet glaciers during deglaciation of the Fennoscandian Ice Sheet: Geology,, doi: 10.1130/G35299.1.

Strand, K., Passchier, S., & Na¨si, J. (2003). Implications of quartz grain microtextures for onset of Eocene/Oligocene glaciation in Prydz Bay, ODP Site 1166, Antarctica. Palaeogeogr. Palaeoclimatol. Palaeoecol., 198, 101–112.

Sugden, D. E., Bentley, M. J., & Cofaigh, C. Ó. (2006). Geological and geomorphological insights into Antarctic ice sheet evolution. *Philosophical Transactions of the Royal Society of London A: Mathematical, Physical and Engineering Sciences*, *364*(1844), 1607-1625.

Swartz, J.M., Gulick, S., and Goff, J.A., 2015, Gulf of Alaska continental slope morphology: Evidence for recent trough mouth fan formation: Geochemistry,, doi: 10.1002/2014GC005594.

Tarasov, L. & Peltier, W. R. Arctic freshwater forcing of the Younger Dryas cold reversal. *Nature* 435, 662–665 (2005).

ten Brink, U., Schneider, C., 1995. Glacial morphology and depositional sequences of the Antarctic continental shelf. Geology 23, 580–584.

Van der Vegt, P., Janszen, A., & Moscariello, A. (2012). Tunnel valleys: current knowledge and future perspectives. *Geological Society, London, Special Publications*, *368*(1), 75-97.

Vorren, T. O., & Laberg, J. S. (1997). Trough mouth fans—palaeoclimate and ice-sheet monitors. *Quaternary Science Reviews*, *16*(8), 865-881.

Vorren, T.O., Laberg, J.S., Blaume, F., Dowdeswell, J.A., Kenyon, N.H., Mienert, J., Rumohr, J., Werner, F., 1998. The Norwegian-Greenland Sea continental mar- gins: morphology and late Quaternary sedimentary processes and environ- ment. Quat. Sci. Rev. 17, 273-302.

Wellner, J.S., Lowe, A.L., Shipp, S.S., Anderson, J.B., 2001. Distribution of glacial geomorphic features on the Antarctic continental shelf and correlation with substrate: implications for ice behavior. J. Glaciol. 47, 397-411.

Wellner, J.S., Heroy, D.C., Anderson, J.B., 2006. The death mask of the Antarctic ice sheet: comparison of glacial geomorphic features across the continental shelf. Geomorphology 75, 157-171.

Wingham, D.J., Siegert, M.J., Shepherd, A., Muir, A.S., 2006. Rapid discharge connects Antarctic subglacial lakes. Nature 440, 1033–1036.

Wright, A. P., et al. (2012), Evidence of a hydrological connection between the ice divide and ice sheet margin in the Aurora Subglacial Basin, East Antarctica, J. Geophys. Res., 117, F01033

Worthington, L., Gulick, S., and Pavlis, T., 2010, Coupled stratigraphic and structural evolution of a glaciated orogenic wedge, offshore St. Elias orogen, Alaska: Tectonics, v. 29, no. 6, p. , doi: 10.1029/2010TC002723.

Young, DA, AP Wright, JL Roberts, and RC Warner (2011), A dynamic early East Antarctic Ice Sheet suggested by ice-covered fjord landscapes, *Nature*. [online] Available from: http://www.nature.com/nature/journal/v474/n7349/abs/nature10114.html

Zachos, J. C., Breza, J. R., & Wise, S. W. (1992). Early Oligocene ice-sheet expansion on Antarctica: Stable isotope and sedimentological evidence from Kerguelen Plateau, southern Indian Ocean. Geology, 20, 569–573.

Zachos, J. C., N. J. Shackleton, J. S. Revenaugh, H. Pälike, and B. P. Flower (2001), Climate response to orbital forcing across the Oligocene-Miocene boundary., *Science*, *292*(5515), 274–8, doi:10.1126/science.1058288

Zhang, S. H., Y. Zhao, X. C. Liu, Y. S. Liu, K. J. Hou, C. F. Li, and H. Ye (2012), U-Pb geochronology and geochemistry of the bedrocks and moraine sediments from the Windmill Islands: Implications for Proterozoic evolution of East Antarctica, Precambrian Res., 206–207, 52–71.

Zwally, H.J., Giovinetto, M.B., Li, J., Cornejo, H.G., Beckley, M.A., Brenner, A.C., Saba, J.L., and Yi, D., 2005, Mass changes to the Greenland and Antarctic ice sheets and shelves and contributions to sea- level rise: 1992-2002, *Journal of Glaciology*, 51, 509-527.